ともに，製剤開発を妨げない規定となるような配慮がなされた。

日局16では，製剤通則には製剤全般に共通する事項や原則のみを記載し，さらに製剤各条の項を設け，医療現場で汎用されている多くの剤形を取り入れるとともに，体系的に分類した。さらに生薬に用いられる剤形（エキス剤，丸剤，酒精剤，浸剤・煎剤，茶剤，チンキ剤，芳香水剤及び流エキス剤）は生薬関連製剤各条として，アイウエオ順に収載することとした（別表1）。

2－1　製剤通則に関して：

容器・包装に関して，日局15では製剤各条に製剤ごとに「本剤に用いる容器は，○○容器とする」と一律に定められていたのに対して，日局16では製剤通則に「製剤の容器・包装は，製剤の品質確保と共に，適正な使用及び投与時の安全確保に適したものとする」との記述が追加され，適正な使用や投与時の安全確保の観点が盛り込まれた。また，薬剤に求められる容器・包装はその薬剤の特性によって異なることから，酸素や湿気，水分の蒸散の影響を受けやすい製剤はそれぞれ保護する特性を有する容器・包装（例えば脱酸素剤の装填や低気体透過性材料の使用）を使用できることとし，柔軟な対応を可能とした。

日局15の製剤通則で言及されていたパラメトリック・リリースの記載が日局16からは削除された。パラメトリック・リリースは，製造工程のバリデーション及び適切な工程管理とその記録の照査により品質を保証する品質管理手法であり，無菌性に関する品質管理の手法として「高度な水準での無菌性が恒常的に保証される場合には，出荷時の試験において，無菌試験を省略することができる」として推奨されていた。削除されても日局16の方針には変わりなく，通則12で工程のバリデーション，工程管理による品質保証と最終製品試験の省略に言及されており，製剤通則の記載は重複になると判断されたためである。

2－2　製剤各条の分類に関して

製剤各条では製剤は，大，中，小に3段階に分けて体系的に分類された。大分類としては，投与経路及び適用部位別に分類し，さらに中分類では，製剤の形状および剤形で分類し，さらに小分類として，機能性やその他の特徴で，適宜分類した。例えば，大分類「経口投与される製剤」では，錠剤，カプセル剤，顆粒剤，散剤等が中分類され，さらに，錠剤の中で，口腔内崩壊錠やチュアブル錠等が小分類されるという，3段階の階層構造となっている。剤形ごとに，定義，製法，製剤品質特性（あるいは規格とその試験法），容器及び包装と貯法が，この順で必要に応じて記載されている。なお，別表1に示された剤形は一般的に使用されているものを示したものであり，これら以外の剤形についても，必要に応じて，適切な剤形とすることができる．例えば，投与経路と製剤各条の剤形名などを組み合わせることにより，形状又は用途などに適した剤形名を使用することができることが，製剤総則の通則に明記されている。

この様に分類することによって，要求される品質特性が類似した剤形は基本的に分類上近い場所に位置するようになった。さらに新しい剤形（口腔内崩壊錠やチュアブル錠）を適切な位置に収載することが可能となった。

剤形に応じた製剤特性を規定することや，製剤特性は適切な試験により確認することが，製剤通則に規定されている。しかし，新たに収載された製剤各条では「適切な○○性を有する」ことが定められてはいるものの，その試験法が日本薬局方一般試験法に定められていない製剤試験も存在する。最終製剤の品質試験よりもむしろ，工程を管理することにより品質を保証してきた製剤もあり，新薬剤の品質試験の日本薬局方一般試験法への取り込みは今後の課題である[2)]。

2－3　定義が変更された剤形

この新たな分類に伴い，顆粒剤・散剤および軟膏・クリーム剤の定義が変更された。品質管理や医療現場での使用に直接関連する製剤の本質を重視したためである。

①顆粒剤・散剤

日局15では，散剤は，「医薬品を粉末又は微粒状に製したもの」であり，製造方法に関しても「適切な方法で粉末又は微粒状とする」ことが記載され，造粒された医薬品も含む定義となっていた。散剤と顆粒剤とを区別するものは，造粒されているか否かでなくその粒子径であり，散剤とは，「製剤の粒度の試験〈6.03〉を行う

とき，18号ふるいを全量通過し，30号ふるいに残留するものは全量の５％ 以下であること」が要件となっていた。

顆粒剤は,「医薬品を粒状に製したものであり，製剤の粒度の試験〈6.03〉を行うとき，10号ふるいを全量通過し，12号ふるいに残留するものは全量の５%以下であり，また，42号ふるいを通過するものは全量の15% 以下である」とされていた。

日局16では，散剤は，経口投与する粉末状の製剤であり，顆粒剤は，経口投与する粒状に造粒した製剤であると定義され，両者の違いは粒子径ではなく，製造過程に造粒プロセスを含むか否かによることとなった。

このように定義を変更した理由は，造粒プロセスを経て製造される顆粒剤では，崩壊過程が溶出に影響を与えることがあるのに対して，散剤では粒子径が溶出性に影響を与えるため，品質管理の観点からは考慮すべき因子が両者で異なるからである[2)]。このように再定義することにより，顆粒剤や散剤の定義に粒度規定を有しないEPやUSPとも整合を図ることができた。

一方，定義を変更すると，既存の医薬品では散剤と称していた医薬品を顆粒剤と変更する必要が生じるため，現行の粒度規定による散剤の定義を救済措置として残している。即ち，顆粒剤の規定の中で「18号ふるいを全量通過し，30号ふるいに残留するものは全量の５％以下のものを散剤と称することができる」とされた。さらに「製剤の粒度の試験法〈6.03〉を行うとき，18号（850μm）ふるいを全量通過し，30号（500μm）ふるいに残留するものは全量の10%以下のものを細粒剤と称することができる」との規定を残し，細粒剤を存続させた。

②軟膏・クリーム

日局15では，軟膏剤は，「通例，適切な稠度の全体を均質な半固形状に製した，皮膚に塗布する外用剤」であると定義され，また，「乳化した基剤を用いたものをクリームと称することができる」として，クリームも軟膏に含めて定義されていた。しかし医療現場では両者は異なる用途で用いられることが多いことから，日局16では軟膏剤とクリーム剤はそれぞれに定義された。即ち，軟膏は，「皮膚に塗布する，有効成分を基剤に溶解又は分散させた半固形の製剤」であるとされ，クリームは「水中油型又は油中水型に乳化した半固形の製剤」とされた。

3．医薬品各条の改正

日局16では生薬を除き，270品目が新規に収載され（添加物２品目を含む），18品目が削除された。表２に新規収載品目の内訳を示す。可能な限り医療上有用な医薬品の収載を目指すという方針に従い，化学薬品を中心に大幅に品目数は増大し，またその約50%は医薬品製剤であった。

日局16では，多くの各条が改正された。その中で最も影響の大きいものは水各条の改正であろう。日局15では製薬用水は常水，精製水，滅菌精製水，注射用水に分類されていたが，日局16では精製水および注射用水にそれぞれ，同（容器入り）が追加され，製薬用水製造システムで製造され，消費されるバルクとしての水と容器に入れて市場に供給される水の２種にわけることとなった。同時に滅菌精製水は滅菌精製水（容器入り）とされた。バルクとして用いられる水は有機不純物含量が低く，容器入りの水とは管理が異なることに対応したものであり，国際的にも整合性が取れたものとなった。水各条の改正に関しては小嶋茂雄博士による優れた総説があるので，そちらを参照していただきたい[3)]。

本稿では製造工程を反映した日本薬局方の取り組みの一例として，異なる製造方法で製造される

表２　日局16における新規収載品目の内訳*1

	化学合成薬品	抗生物質	生物薬品	合計
原薬	113	2	3	118
製剤	114	36	0	150
合計	227	38	3	268

*1 日局15から新たに収載された品目数，ただし生薬および添加物を除く

医薬品が存在する場合の各条における取扱を紹介したい。

3－1 異なる製造方法で製造される医薬品が存在する場合の各条における取扱

冒頭に述べたように，日本薬局方は規格・基準及び標準的試験法等を示す公的な規範書であり，その内容は公開され，公共のものとなるべきものである。一方，品質特性の中には，個別医薬品の製造方法に依存し，一つに特定することが適当でない場合も存在する。日本薬局方は，そのような場合に医薬品各条の試験では「別に規定する」とし，具体的な事項は薬事法に基づく承認の際に規定する余地を残している。日局16では医薬品原薬の残留溶媒および結晶多形について，製造方法に依存して製品によって異なる場合があるので,「別に規定する」として，異なる特性を持つ医薬品の存在を許容することとしたので，以下に記述する。

①残留溶媒の取り扱い

化学合成医薬品は製造工程で有機溶媒を使用し，最終原薬に持ち込まれ残存するケースが多く，残存する有機溶媒の種類は最終精製工程で使用する溶媒より主に決定される。残留溶媒は患者にとってベネフィットはないので，ICHガイドラインで，その残留溶媒のヒト健康へのリスクに応じて許容量が厳しく規制されている。日本薬局方は日局15第２追補から，有機溶媒を製造工程で使用している原薬に関しては，残留溶媒を規制することとし，その際に一律に残留する溶媒の種類と量を規定するのではなく,「別に規定する」とした。第16改正では計73品目に残留溶媒が「別に規定する」として設定された。

②結晶多形の取り扱い

化学合成医薬品原薬の中には結晶多形が存在するものが多い。結晶多形とは同一分子でありながら結晶中での分子の配列の仕方が異なるものをいう（日本薬学会薬学用語解説より）。それぞれの結晶多形が存在する場合，結晶構造の違いにより，溶解性，安定性や製造性が異なる場合が存在する。

近年，医薬品産業は，安定性や溶解性に大きな影響を与える結晶構造に関して，知的所有権を求め，特許を取得するケースが増大した。このような場合，たとえ先発会社の医薬品の物質特許が失効していても，結晶多形に関する特許が有効である場合，日本薬局方に収載することが困難になる。何故ならば，日本薬局方は原薬の確認試験として，分子の構造のみならず，結晶構造を特定しうる試験方法である赤外吸収スペクトル測定法を採用してきたため，赤外吸収スペクトルにより結晶多形が先発会社の結晶形に限定されてしまい，局方に収載すると，製造会社が限定されてしまうからである。

結晶多形は溶出性等に影響するものの，一旦溶解してしまえば，結晶多形による違いはなく，同一の生物活性が期待されるはずである。さらに溶出性や安定性は製剤技術の改良により補うことが可能であることから，日局16では，結晶多形に特許が存在する７品目（サルポグレラート塩酸塩，ラベプラゾールナトリウム，アトルバスタチンカルシウム水和物，カンデサルタンシレキセチル，ドネペジル塩酸塩，ナテグリニド，フェキソフェナジン塩酸塩）に関して複数の結晶多形が許容できる方策を講じた。例えばアトルバスタチンカルシウム水和物以下の５品目に関しては，スペクトルに差を認めるときは別に規定する方法により再結晶し，結晶をろ取し，乾燥したものにつき同様の試験（IR 試験）を行うこととして，結晶多形を変換して測定することが可能とした。なお，製造会社は自社で定めた特定の結晶形の原薬を恒常的に製造する必要があり，そのために自社の原薬の結晶多形の一貫性を保証可能な（自社の結晶多形を社内標準物質に設定するなど）試験方法を設定する必要がある。

4．おわりに

日本薬局方は1886年（明治19年）に第一版が発行されて以来，その間15回の大改訂を行い，今年で125年目を迎えた。日局16の収載品目数は1764品目であり，日局15に比べても281品目の増加である（なお，第一版は468品目）。単に各条品目が増えただけでなく，今回は実に50年ぶりに製剤総則が大幅に改正された。この改正により日本薬局方の製剤の分類は科学的・合理的になり，国際的にも整合性のある分類となった。

医薬品各条の記載内容も変わりつつある。管理しなければならない品質特性の中で，製造方法の

違いにより単一には定められない特性は，個別承認に委ねられるケースが増大した。医薬品品質の管理手法は，科学技術の進歩（例えば非破壊分析による工程内管理など）に伴い，多様化しつつあり，日本薬局方も次回（あるいはその後も視野に入れて）の大改訂に向けて準備を開始しつつある。

日本薬局方は薬事法41条で定められた公的な規格基準書であり，医療，教育，生産等の様々な場面で活用されることを期待している。

参考文献

1）平成18年７月26日　薬事・食品衛生審議会答申「第十六改正日本薬局方作成基本方針」(http://www.mhlw.go.jp/topics/bukyoku/iyaku/yakkyoku/)
2）青柳伸男，医薬品研究39，741-759 (2008)
3）小嶋茂雄，PHARMA TECH JAPAN 27 1519-1534 (2011)

別表１　第16改正日本薬局方による製剤の分類（生薬関連製剤を除く）

1.経口投与する製剤 (Preparations for Oral Administration)
- 1.1.錠剤 (Tablets)：経口投与する一定の形状の固形の製剤
  - 1.1.1.口腔内崩壊錠 (Orally Disintegrating Tablets/Orodispersible Tablets)：口腔内で速やかに溶解又は崩壊させて服用できる錠剤
  - 1.1.2.チュアブル錠 (Chewable Tablets)：咀嚼して服用する錠剤
  - 1.1.3.発泡錠 (Effervescent Tablets)：水中で急速に発泡しながら溶解又は分散する錠剤
  - 1.1.4.分散錠 (Dispersible Tablets)：水に分散して服用する錠剤
  - 1.1.5.溶解錠 (Soluble Tablets)：水に溶解して服用する錠剤
- 1.2.カプセル剤 (Capsules)：経口投与する，カプセルに充てん又はカプセル基剤で被包成形した製剤
- 1.3.顆粒剤 (Granules)：経口投与する粒状に造粒した製剤
  - 1.3.1.発泡顆粒 (Effervescent Granules)：水中で急速に発泡しながら溶解又は分散する顆粒剤
- 1.4.散剤 (Powders)：経口投与する粉末状の製剤
- 1.5.経口液剤 (Liquids and Solutions for Oral Administration)：経口投与する，液状又は流動性のある粘稠なゲル状の製剤
  - 1.5.1.エリキシル剤 (Elixirs)：甘味及び芳香のあるエタノールを含む澄明な液状の経口液剤
  - 1.5.2.懸濁剤 (Suspensions)：有効成分を微細均質に懸濁した経口液剤
  - 1.5.3.乳剤 (Emulsion)：有効成分を微細均質に乳化した経口液剤
  - 1.5.4.リモナーデ剤 (Lemonades)：甘味及び酸味のある澄明な液状の経口液剤
- 1.6.シロップ剤 (Syrups)：経口投与する，糖類又は甘味剤を含む粘稠性のある液状又は固形（シロップ用剤）の製剤
  - 1.6.1.シロップ用剤 (Preparations for Syrups)：水を加えるとき，シロップ剤となる顆粒状又は粉末状の製剤
- 1.7.経口ゼリー剤 (Jellies for Oral Administration)：経口投与する，流動性のない成形したゲル状の製剤

2.口腔内に適用する製剤 (Preparations for Oro-mucosal Application)
- 2.1.口腔用錠剤 (Tablets for Oro-mucosal Application)：口腔内に適用する一定の形状の固形の製剤
  - 2.1.1.トローチ剤 (Troches/Lozenges)：口腔内で徐々に溶解又は崩壊させ，口腔，咽頭などの局所に適用する口腔用錠剤
  - 2.1.2.舌下錠 (Sublingual Tablets)：有効成分を舌下で速やかに溶解させ，口腔粘膜から吸収させる口腔用錠剤
  - 2.1.3.バッカル錠 (Buccal Tablets)：有効成分を臼歯と頬の間で徐々に溶解させ，口腔粘膜か

ら吸収させる口腔用錠剤
2.1.4.付着錠（Mucoadhesive Tablets）：口腔粘膜に付着させて用いる口腔用錠剤
2.1.5.ガム剤（Medicated Chewing Gums）：咀嚼により，有効成分を放出する口腔用錠剤
2.2.口腔用スプレー剤（Sprays for Oro-mucosal Application）：口腔内に適用する，有効成分を霧状，粉末状，泡沫状又はペースト状などとして噴霧する製剤
2.3.口腔用半固形剤（Semi-solid Preparations for Oro-mucosal Application）：口腔粘膜に適用するクリーム剤，ゲル剤又は軟膏剤
2.4.含嗽剤（Preparations for Gargles）：口腔，咽頭などの局所に適用する液状の製剤

3.注射により投与する製剤（Preparations for Injection）
3.1.注射剤（Injections）：皮下，筋肉内又は血管などの体内組織・器官に直接投与する，通例，溶液，懸濁液若しくは乳濁液，又は用時溶解若しくは用時懸濁して用いる固形の無菌製剤
3.1.1.輸液剤（Parenteral Infusions）：静脈内投与する，通例，100mL以上の注射剤
3.1.2.埋め込み注射剤（Implants/Pellets）：長期にわたる有効成分の放出を目的として，皮下，筋肉内などに埋め込み用の器具を用いて，又は手術により適用する固形又はゲル状の注射剤
3.1.3.持続性注射剤（Prolonged Release Injections）：長期にわたる有効成分の放出を目的として，筋肉内などに適用する注射剤

4.透析に用いる製剤（Preparations for Dialysis）
4.1.透析用剤（Dialysis Agents）：腹膜透析又は血液透析に用いる液状若しくは用時溶解する固形の製剤
4.1.1.腹膜透析用剤（Peritoneal Dialysis Agents）：腹膜透析に用いる無菌の透析用剤
4.1.2.血液透析用剤（Hemodialysis Agents）：血液透析に用いる透析用剤

5.気管支・肺に適用する製剤（Preparations for Inhalation）
5.1.吸入剤（Inhalations）：有効成分をエアゾールとして吸入し，気管支又は肺に適用する製剤.
5.1.1.吸入粉末剤（Dry Powder Inhalers）：吸入量が一定となるように調製された，固体粒子のエアゾールとして吸入する製剤
5.1.2.吸入液剤（Inhalation Solutions）：ネブライザなどにより適用する液状の吸入剤
5.1.3.吸入エアゾール剤（Metered-Dose Inhalers）：容器に充てんした噴射剤と共に，一定量の有効成分を噴霧する定量噴霧式吸入剤

6.目に投与する製剤（Preparations for Ophthalmic Application）
6.1.点眼剤（Ophthalmic Preparations）：結膜嚢などの眼組織に適用する，液状，又は用時溶解若しくは用時懸濁して用いる固形の無菌製剤
6.2.眼軟膏剤（Ophthalmic Ointments）：結膜嚢などの眼組織に適用する半固形の無菌製剤

7.耳に投与する製剤（Preparations for Otic Application）
7.1.点耳剤（Ear Preparations）：外耳又は中耳に投与する，液状，半固形又は用時溶解若しくは用時懸濁して用いる固形の製剤

8.鼻に適用する製剤（Preparations for Nasal Application）
8.1.点鼻剤（Nasal Preparations）：鼻腔又は鼻粘膜に投与する製剤

8.1.1.点鼻粉末剤（Nasal Dry Powder Inhalers）：鼻腔に投与する微粉状の点鼻剤
8.1.2.点鼻液剤（Nasal Solutions）：鼻腔に投与する液状，又は用時溶解若しくは用時懸濁して用いる固形の点鼻剤

9.直腸に適用する製剤（Preparations for Rectal Application）
9.1.坐剤（Suppositories for Rectal Application）：直腸内に適用する，体温によって溶融するか，又は水に徐々に溶解若しくは分散することにより有効成分を放出する一定の形状の半固形の製剤
9.2.直腸用半固形剤（Semi-solid Preparations for Rectal Application）：肛門周囲又は肛門内に適用するクリーム剤，ゲル剤又は軟膏剤
9.3.注腸剤（Enemas for Rectal Application）：肛門を通して適用する液状又は粘稠なゲル状の製剤

10.腟に適用する製剤（Preparations for Vaginal Application）
10.1.腟錠（Tablets for Vaginal Use）：腟に適用する，水に徐々に溶解又は分散することにより有効成分を放出する一定の形状の固形の製剤
10.2.腟用坐剤（Suppositories for Vaginal Use）：腟に適用する，体温によって溶融するか，又は水に徐々に溶解若しくは分散することにより有効成分を放出する一定の形状の半固形の製剤

11.皮膚などに適用する製剤（Preparations for Cutaneous Application）
11.1.外用固形剤（Solid Dosage Forms for Cutaneous Application）：皮膚（頭皮を含む）又は爪に，塗布又は散布する固形の製剤
11.1.1. 外用散剤（Powders for Cutaneous Application）：粉末状の外用固形剤
11.2.外用液剤（Liquids and Solutions for Cutaneous Application）：皮膚（頭皮を含む）又は爪に塗布する液状の製剤
11.2.1.リニメント剤（Liniments）：皮膚にすり込んで用いる液状又は泥状の外用液剤
11.2.2.ローション剤（Lotions）：有効成分を水性の液に溶解又は乳化若しくは微細に分散させた外用液剤
11.3. スプレー剤（Sprays for Cutaneous Application）：有効成分を霧状，粉末状，泡沫状，又はペースト状などとして皮膚に噴霧する製剤
11.3.1. 外用エアゾール剤（Aerosols for Cutaneous Application）：容器に充てんした液化ガス又は圧縮ガスと共に有効成分を噴霧するスプレー剤
11.3.2. ポンプスプレー剤（Pump Sprays for Cutaneous Application）：ポンプにより容器内の有効成分を噴霧するスプレー剤
11.4.軟膏剤（Ointments）：皮膚に塗布する，有効成分を基剤に溶解又は分散させた半固形の製剤
11.5.クリーム剤（Creams）：皮膚に塗布する，水中油型又は油中水型に乳化した半固形の製剤
11.6.ゲル剤（Gels）：皮膚に塗布するゲル状の製剤
11.7.貼付剤（Patches）：皮膚に貼付する製剤
11.7.1.テープ剤（Tapes/Plasters）：ほとんど水を含まない基剤を用いる貼付剤
11.7.2.パップ剤（Cataplasms/Gel Patches）：水を含む基剤を用いる貼付剤

Rapid and Sensitive Method for Measuring the Plasma Concentration of Doxorubicin and Its Metabolites

Kumiko Sakai-Kato,*[a] Kunie Nanjo,[a] Toru Kawanishi,[b] and Haruhiro Okuda[a]

[a] *Division of Drugs, National Institute of Health Sciences; and* [b] *National Institute of Health Sciences; 1–18–1 Kamiyoga, Setagaya-ku, Tokyo 158–8501, Japan.*

Received September 9, 2011; accepted December 16, 2011; published online December 21, 2011

Doxorubicin is an anti-cancer drug with a wide therapeutic range. However, it and its metabolites cause severe side effects, limiting its clinical use. Therefore, measuring the plasma concentration of doxorubicin and its metabolites is important to study the dosing regimen of doxorubicin. We developed a rapid and sensitive method by ultra-high-performance liquid chromatography with fluorescent detection for measuring the plasma concentration of doxorubicin and its metabolites in small volumes (around 10 μL), enabling repeated measurements from the same mouse. The sensitivity of 7-deoxydoxorubicinolone, a major metabolite of doxorubicin, increased about 5 times than those ever reported using conventional HPLC, and the run time was within 3 min. The area under the curve ($AUC_{0-24\,h}$) of doxorubicin was 5.9 μg h/mL similar to the value of 4.16 μg h/mL obtained previously using a conventional HPLC method. This method would provide information that could be used to refine the therapeutic approach to doxorubicin use.

Key words doxorubicin; metabolite; pharmacokinetics

The anthracycline doxorubicin is one of the most widely used anticancer agents, and it has a broad spectrum of activity against a variety of malignancies.[1,2] New formulation technologies to enhance the effectiveness and safety of this anticancer drug are currently being developed. For instance, long-circulating and sterically stabilized liposomes containing doxorubicin can markedly increase tumor-specific deposition of drugs and have been approved as clinical products.[3] However, the clinical use of doxorubicin is limited by the side effect of cumulative, dose-dependent, irreversible chronic cardiomyopathy caused by doxorubicin itself and its metabolites, and optimal dose schedules remain a matter of debate.[4] Therefore, measuring the plasma concentration of doxorubicin and its metabolites is important to study the dosing regimen of doxorubicin.

Mice are very useful small laboratory animals for nonclinical research and are often used for pharmacokinetic, pharmacological, or drug formulation studies of doxorubicin.[5—7] Blood collection from the tail vein is becoming popular from the perspective of animal protection, but it has the limitation of small sample volumes. Therefore, it is often difficult to perform repeat investigations in the same animal to assess time-dependent changes in plasma concentrations, and many mice have to be killed for whole blood collection at each time point.

In a previous study, we succeeded in developing a method for measuring intracellular concentrations of doxorubicin and its metabolites by using ultra-high-performance liquid chromatography (UHPLC).[8] The resolution, sensitivity, and speed of analysis dramatically increased with the use of 2-μm particles in the stationary phase, high linear velocities for the mobile phase, and instrumentation that operates at higher pressures than those used in HPLC.[9—11] Specifically, the quantitation limit of doxorubicin was about 2 times lower than the limit ever reported using conventional HPLC, and run time was shorten from 20 min to within 3 min,[12,13] Because of the high sensitivity of our method and the small sample volumes (around 10 μL) required, in the current study we were able to measure changes in the concentration of doxorubicin and its metabolites over time in a single mouse, thereby diminishing the number of animals needed. This method would also have clinical utility, because the reduction of sample volumes and analytical times would decrease the burden of therapeutic drug monitoring (TDM) for patients.

Experimental

Drugs and Chemicals Doxorubicin hydrochloride, daunorubicin hydrochloride, and verapamil were purchased from Wako Pure Chemical Industries, Ltd. (Osaka, Japan). Doxorubicinol hydrochloride, and 7-deoxydoxorubicinolone were purchased from Toronto Research Chemicals Inc. (North York, Canada). Doxorubicinolone was synthesized from doxorubicinol by acidic hydrolysis (0.5 N HCl) at 50°C for 24 h, and then extracted with chloroform by a liquid–liquid extraction method.[14] Stock solution of each chemical was prepared by weighing separately. The primary stock solution of each chemical was prepared in methanol at 0.35 or 0.1 mg/mL and stored at −80°C. The standard solutions for validation data were obtained by mixing each chemical with mouse blank plasma.

Preparation of Mouse Plasma Samples for HPLC Doxorubicin was administered at 10 mg/kg by tail vein injection into female Balb/c mice purchased from CLEA Japan, Inc. (Tokyo, Japan). Blood was collected from the tail vein into heparinized capillaries 10, 20, 40, and 60 min and 2, 6, and 24 h after doxorubicin administration. Plasma obtained from the blood sample (about 10 μL) was mixed with saline, 50% methanol, and $ZnSO_4$ (final concentration: 400 mg/mL) and centrifuged at 15000 *g* for 10 min in a microcentrifuge (Model 3740, Kubota Corp., Tokyo, Japan); the supernatants were then collected. Plasma and saline volumes were adjusted so that the concentration of each compound was within the calibration curve range. A 15-μL aliquot of each supernatant was mixed with 5 μL of the internal standard (daunorubicin, 10 μg/mL in methanol), 22.5 μL ice-cold methanol, and 7.5 μL Milli-Q water, and filtered through a 0.20-μm filter (Millex-LG, Millipore Corp., Tokyo, Japan). The filtrates were transferred to autosampler vials before UHPLC analysis. All experimental procedures were approved by the institutional

* To whom correspondence should be addressed. e-mail: kumikato@nihs.go.jp

animal care and use committee.

HPLC Conditions High-throughput quantification of doxorubicin and its metabolites was performed in a Hitachi LaChrom ULTRA system equipped with an L-2160U pump, an L-2200U automated sample injector, an L-2300 thermostatted column compartment, and an L-2485U fluorescence detector (Hitachi, Tokyo, Japan).[8]

Samples were analyzed on a Capcell Pak C18 IF column (2.0×50 mm; particle size, 2 μm; Shiseido Corp., Tokyo, Japan). The mobile phase consisted of a mixture of 50 mM sodium phosphate buffer (pH 2.0) and acetonitrile (65 : 27, v/v). The mobile phase was delivered at a rate of 300 μL/min, and the column temperature was maintained at 25°C. The fluorescence detector was operated at an excitation wavelength of 470 nm and an emission wavelength of 590 nm.

Pharmacokinetics Analysis Pharmacokinetics were analyzed by noncompartmental analysis using Phoenix WinNonlin V6.1 software (Pharsight Corporation, CA, U.S.A.).

Results and Discussion

Doxorubicin is mainly metabolized in liver, and the estimated metabolic pathway was shown in Fig. 1a. According to a report where human metabolism of doxorubicin was studied

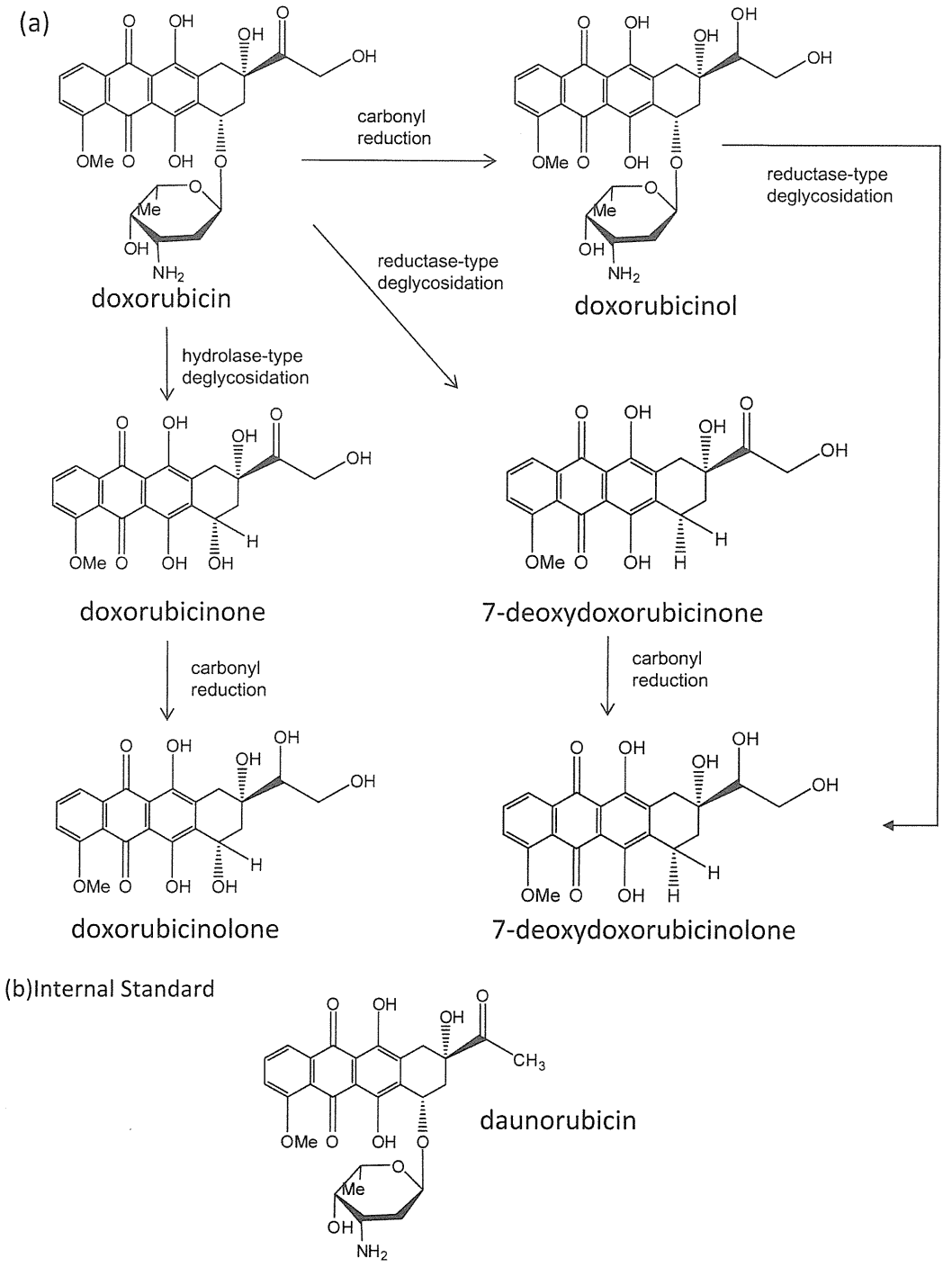

Fig. 1. Schematic Showing the Chemical Structures of Doxorubicin and Its Metabolites (a) and the Chemical Structure of Daunorubicin, the Internal Standard (b)

Table 1. Linearity of Doxorubicinone and Its Metabolites

	Slope			Intercept		r^2
	Mean	S.D.	Precision (%)	Mean	S.D.	
Doxorubicinol	12.71	0.22	1.73	0.0012	0.0062	1.000
Doxorubicin	12.16	0.19	1.56	−0.0009	0.0026	1.000
Doxorubicinolone	10.89	0.22	2.04	0.0029	0.0073	0.999
7-Deoxydoxorubicinolone	14.07	0.31	2.20	0.0049	0.0069	0.999

Precision (%): expressed as % R.S.D. (S.D./mean)×100.

Table 2. Detection Limit and Quantification Limit of Doxorubicin and Its Metabolites

	Doxorubicinol	Doxorubicine	Doxorubicinolone	7-Deoxydoxorubicinolone
Detection limit (pg)	3.8	4.9	6.4	7.4
Quantification limit (pg)	12.8	16.4	21.4	24.5

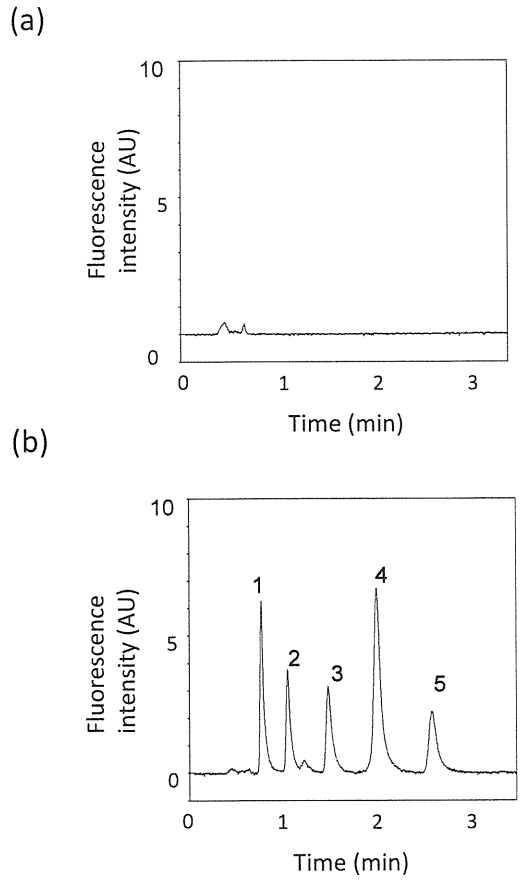

Fig. 2. Chromatograms of (a) Mouse Plasma and (b) Mouse Plasma Spiked with Doxorubicin and Its Metabolites

The chromatographic conditions are described in Experimental. AU; Arbitrary units. 1, doxorubicinol; 2, doxorubicin; 3, doxorubicinolone; 4, daunorubicin (internal standard); 5, 7-deoxydoxorubicinolone.

by isolating and identifying urinary metabolites, the metabolites retained doxorubicin's specific fluorescence properties.[15] Therefore, in this report, we used the fluorescent detection condition optimized for doxorubicin. Although the metabolites in human urine contained sulfate and glucuronide conjugates, which conjugate reactions also occur in liver, these conjugates were not detected in mouse plasma in our study. When a standard solution of doxorubicin, doxorubicinol, doxorubicinolone, 7-deoxydoxorubicinolone, and an internal standard (daunorubicin (Fig. 1b)) was analyzed, all compounds were separated within 3 min with good resolution (Fig. 2). The chromatogram of mouse plasma demonstrates the lack of chromatographic interference from endogenous plasma components (Fig. 2a). In a chromatogram of plasma spiked with doxorubicin and its metabolites at a concentration of 20 ng/mL, no interfering peaks were observed, and doxorubicin, the three metabolites, and the internal standard were well separated (Fig. 2b). These results show that the specificity of this method. We created calibration plots for doxorubicin and its metabolites. The plasma calibration curve was constructed using six calibration standards (2.5—100 ng/mL). The plots of relative peak area to IS *versus* concentration were linear over a wide range of concentrations (r^2=0.999—1.000) (Table 1). The detection limit and quantification limit were 3.8—7.4 pg and 12.8—24.5 pg injected compounds, respectively (signal to noise ratio, 3 : 1 for detection limits and 10 : 1 for quantitation limit). These values were 5 times lower than the limits ever reported using conventional HPLC[12,13,16—19] (Table 2).

We next tested the recovery of doxorubicin and its metabolites from mouse plasma spiked with each compound. The recovery rate was satisfactory, and the values for doxorubicinol, doxorubicin, doxorubicinolone, and 7-deoxydoxorubicinolone were 102.7, 92.6, 94.7, 96.7%, respectively (n=3). Tables 3 and 4 shows the accuracy and precision data for intra- and inter-day plasma samples. The assay values on both occasions (intra- and inter-day) were found to be within the accepted variable limits.[20]

The predicted concentrations for each analyte deviated within ±15% of the nominal concentrations in a series of stability test; in-injector (20 h), bench top (6 h), repeated three freeze/thaw cycles and at −80°C for at least 2 weeks (Table 5). Although 7-deoxydoxorubicinolone was slightly unstable under in-injector (20 h; 91.24%), other compounds were stable at any storage conditions.

We then used the validated method described above for the simultaneous detection of doxorubicin and its metabolites in mouse plasma after intravenous administration of doxorubicin. Doxorubicin and its metabolites doxorubicinol and 7-deoxydoxorubicinolone were detected in the plasma sample. Although doxorubicinolone has been also reported to be produced by NADP-dependent cytochrome P450 reductase,[13,15] it was not detected in this study (Fig. 3). Doxorubicinol is produced by cytosolic carbonyl reductase through the

Table 3. Intra-Day Assay Precision and Accuracy for Doxorubicin and Its Metabolites in Mouse Plasma

ng/mL	Doxorubicinol				Doxorubicin				Doxorubicinolone				7-Deoxydoxorubicinolone			
	Mean	S.D.	Precision	Accuracy	Mean	S.D.	Precision	Accuracy	Mean	S.D.	Precision	Accuracy	Mean	S.D.	Precision	Accuracy
5	5.12	0.41	8.08	102.45	4.98	0.15	3.03	99.56	4.82	0.61	12.73	96.30	4.70	0.44	9.42	93.90
25	25.16	1.40	5.55	100.63	25.46	0.88	3.47	101.84	23.56	1.39	5.92	94.24	25.75	1.25	4.84	102.99
100	99.78	0.94	0.94	99.78	99.55	0.99	1.00	99.55	99.49	1.21	1.22	99.49	99.47	1.13	1.14	99.47

Precision (%): expressed as % R.S.D. (S.D./mean)×100. Accuracy (%): calculated as (mean determined concentration/nominal concentration)×100.

Table 4. Inter-Day Assay Precision and Accuracy for Doxorubicin and Its Metabolites in Mouse Plasma

ng/mL	Doxorubicinol				Doxorubicin				Doxorubicinolone				7-Deoxydoxorubicinolone			
	Mean	S.D.	Precision	Accuracy	Mean	S.D.	Precision	Accuracy	Mean	S.D.	Precision	Accuracy	Mean	S.D.	Precision	Accuracy
5	5.13	0.16	3.04	102.51	5.35	0.49	9.18	107.05	5.31	0.35	6.55	106.18	4.95	0.11	2.25	98.95
25	24.31	0.68	2.81	97.24	23.74	0.38	1.59	94.96	24.84	0.42	1.69	99.34	24.56	0.37	1.52	98.24
100	99.83	0.48	0.48	99.83	100.11	1.13	1.13	100.11	100.39	0.32	0.32	100.39	99.83	0.44	0.44	99.83

Precision (%): expressed as % R.S.D. (S.D./mean)×100. Accuracy (%): calculated as (mean determined concentration/nominal concentration)×100.

Table 5. Stability Data in Mouse Plasma

	Doxorubicinol				Doxorubicin				Doxorubicinolone				7-Deoxydoxorubicinolone			
	Mean	S.D.	Precision	Accuracy	Mean	S.D.	Precision	Accuracy	Mean	S.D.	Precision	Accuracy	Mean	S.D.	Precision	Accuracy
5 ng/mL																
20 h (in-injector)	5.00	0.068	1.37	100.06	5.22	0.072	1.37	104.30	5.19	0.058	1.12	103.86	4.56	0.074	1.62	91.24
6 h (bench-top)	5.19	0.10	2.01	103.71	5.43	0.11	2.08	108.66	5.22	0.11	2.01	104.38	4.92	0.073	1.48	98.39
2 weeks at −80°C	4.72	0.12	2.43	94.36	5.23	0.14	2.62	104.54	5.21	0.082	1.58	104.20	4.98	0.092	1.84	99.59
3rd freeze-thaw	4.80	0.17	3.49	96.00	5.16	0.18	3.51	103.23	5.01	0.22	4.48	100.19	4.97	0.154	3.09	99.42
50 ng/mL																
20 h (in-injector)	51.27	1.48	2.89	102.53	54.10	2.07	3.82	108.20	47.08	1.54	3.28	94.16	50.69	1.77	3.49	101.38
6 h (bench-top)	53.78	2.90	5.39	107.55	52.12	2.76	5.30	104.25	49.66	2.27	4.56	99.32	54.33	2.36	4.33	108.66
2 weeks at −80°C	47.75	0.54	1.13	95.49	48.10	0.47	0.97	96.21	49.04	0.35	0.71	98.08	47.99	0.44	0.91	95.98
3rd freeze-thaw	52.09	0.81	1.56	104.18	51.04	0.81	1.59	102.08	48.68	0.95	1.96	97.37	51.52	0.86	1.68	103.04

Precision (%): expressed as % R.S.D. (S.D./mean)×100. Accuracy (%): calculated as (mean determined concentration/nominal concentration) ×100.

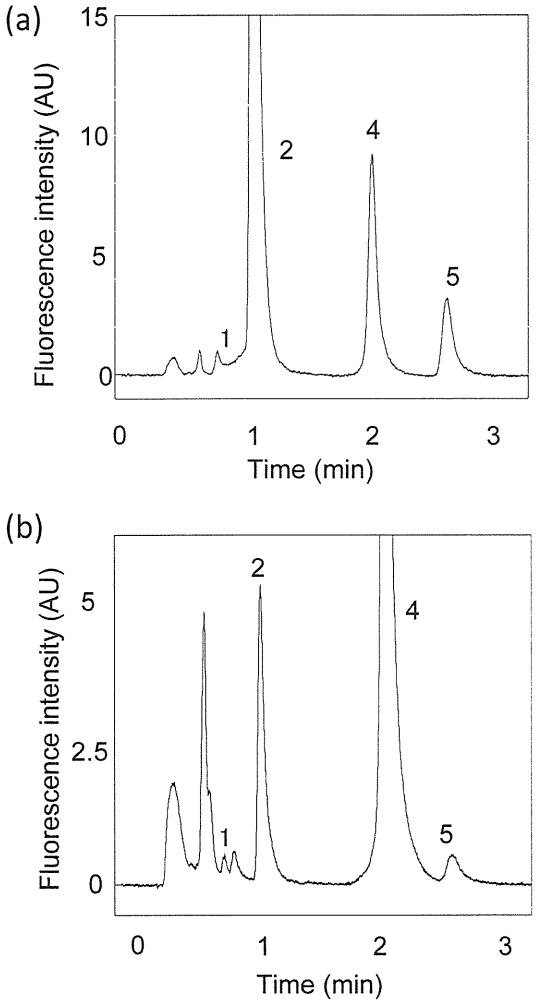

Fig. 3. Chromatogram of Mouse Plasma Obtained after Intravenous Administration of Doxorubicin

Doxorubicin (10 mg/kg) was administered by tail vein injection. Blood was removed from the tail vein after 10 min (a) and 6 h (b) of administration, and plasma was prepared as described in Experimental. 1, doxorubicinol; 2, doxorubicin; 4, daunorubicin (internal standard); 5,7-deoxydoxorubicinolone.

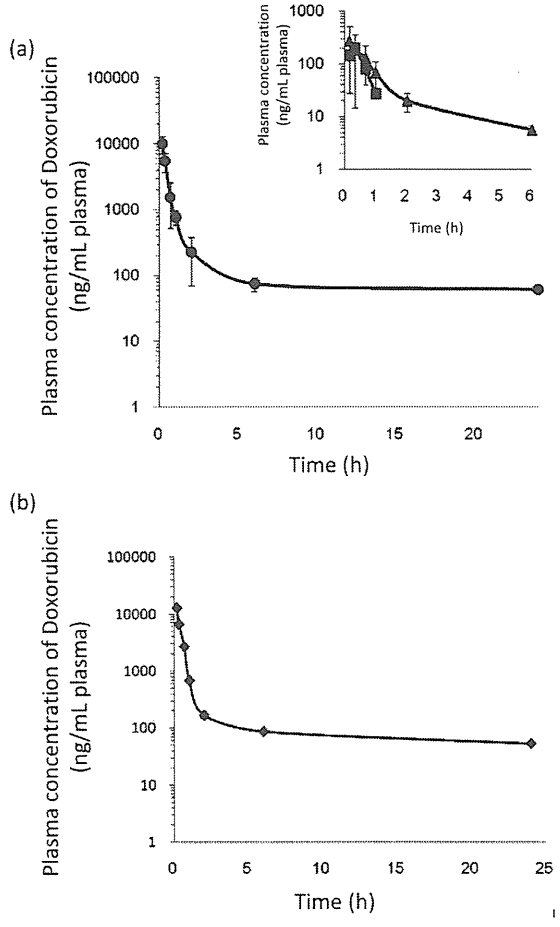

Fig. 4. Changes in Plasma Concentration over Time

Blood was collected from tail veins 10, 20, or 30 min or 1, 2, 6, or 24 h after administration of doxorubicin, and the drug concentrations in the plasma were measured. (Averaged results from 3 mice (a) and result of one mouse (b).) Main graph, doxorubicin. Inset, metabolites (squares: doxorubicinol; triangles: 7-deoxydoxorubicinolone).

NADPH-dependent aldo-keto reduction of a carbonyl moiety in doxorubicin[15]; deglycosidation at the daunosamine sugar in doxorubicin or doxorubicinol produces 7-deoxydoxorubicinolone[15,21] (Fig. 1a). The major metabolites we detected were coincident with those reported previously.[22] We also examined the time course of changes in the concentrations of doxorubicin and its metabolites (Fig. 4a). After an initial rapid decrease, the doxorubicin concentration decreased slowly, and the plasma concentration of doxorubicin was 74.2 ng/mL (6 h) and 61.1 ng/mL (24 h) (n=3). The persistence of doxorubicin indicates that doxorubicin comes back very slowly from some distributed tissues or circulates for a relatively long time by binding to plasma proteins.[15]

The area under the curve (AUC_{0-24h}) and C_{max} of doxorubicin was 5.9 μg h/mL and 10.0 μg/mL, respectively, similar to the value of 4.16 μg h/mL, and 5.4 μg/mL obtained previously using a conventional HPLC method.[7] In addition, our method enabled us to trace the change in doxorubicin concentration over time in a single mouse (Fig. 4b); this had previously been difficult to do because of the small sample volumes. This property will allow us to minimize the number of animals needed for pharmacokinetic analyses. Furthermore, in a clinical setting, the small blood sample volumes and fast analytical time would reduce the impact of TDM on patients.

Conclusions

Our results show that the method we developed using UHPLC provides rapid analysis using very small plasma samples. The method is sensitive enough to evaluate changes in the concentrations of doxorubicin and its metabolites in a single mouse; this will result in the use of smaller numbers of animals, which is good for animal protection. In clinical applications, this method could also decrease the burden of TDM for patients. We predict that it will greatly facilitate studies of doxorubicin pharmacokinetics and clarify the effect of doxorubicin metabolism on therapeutic outcome.

Acknowledgements The authors are grateful for financial support from the Research on Publicly Essential Drugs and Medical Devices Project (The Japan Health Sciences Foundation); a Health Labor Sciences Research Grant from the Ministry of Health, Labour, and Welfare (MHLW); and KAKENHI (21790046) from the Ministry of Education, Culture, Sports, Science and Technology (MEXT) of Japan.

References

1) Hortobágyi G. N., *Drugs*, **54** (Suppl. 4), 1—7 (1997).
2) Di Marco A., Gaetani M., Scarpinato B., *Cancer Chemother. Rep.*, **53**, 33—37 (1969).
3) O'Brien M. E., Wigler N., Inbar M., Rosso R., Grischke E., Santoro A., Catane R., Kieback D. G., Tomczak P., Ackland S. P., Orlandi F., Mellars L., Alland L., Tendler C., CAELYX Breast Cancer Study Group, *Ann. Oncol.*, **15**, 440—449 (2004).
4) Olson R. D., Mushlin P. S., Brenner D. E., Fleischer S., Cusack B. J., Chang B. K., Boucek R. J. Jr., *Proc. Natl. Acad. Sci. U.S.A.*, **85**, 3585—3589 (1988).
5) van Asperen J., van Tellingen O., Beijnen J. H., *Drug Metab. Dispos.*, **28**, 264—267 (2000).
6) Yokoyama M., Okano T., Sakurai Y., Fukushima S., Okamoto K., Kataoka K., *J. Drug Target.*, **7**, 171—186 (1999).
7) Nakanishi T., Fukushima S., Okamoto K., Suzuki M., Matsumura Y., Yokoyama M., Okano T., Sakurai Y., Kataoka K., *J. Controlled Release*, **74**, 295—302 (2001).
8) Sakai-Kato K., Saito E., Ishikura K., Kawanishi T., *J. Chromatogr. B Analyt. Technol. Biomed. Life Sci.*, **878**, 1466—1470 (2010).
9) Swartz M. E., *J. Liq. Chrom. Rel. Technol.*, **28**, 1253—1263 (2005).
10) Nováková L., Vlcková H., *Anal. Chim. Acta*, **656**, 8—35 (2009).
11) Sun N., Lu G., Lin M., Fan G., Wu Y., *Talanta*, **78**, 506—512 (2009).
12) van Asperen J., van Tellingen O., Beijnen J. H., *J. Chromatogr. B Biomed. Sci. Appl.*, **712**, 129—143 (1998).
13) Zhou Q., Chowbay B., *J. Pharm. Biomed. Anal.*, **30**, 1063—1074 (2002).
14) Maudens K. E., Stove C. P., Lambert W. E., *J. Sep. Sci.*, **31**, 1042—1049 (2008).
15) Takanashi S., Bachur N. R., *Drug Metab. Dispos.*, **4**, 79—87 (1976).
16) Andersen A., Warren D. J., Slørdal L., *Ther. Drug Monit.*, **15**, 455—461 (1993).
17) Shinozawa S., Mimaki Y., Araki Y., Oda T., *J. Chromatogr.*, **196**, 463—469 (1980).
18) Rose L. M., Tillery K. F., el Dareer S. M., Hill D. L., *J. Chromatogr.*, **425**, 419—423 (1988).
19) Andersen A., Holte H., Slørdal L., *Cancer Chemother. Pharmacol.*, **44**, 422—426 (1999).
20) Guidance for Industry: Bioanalytical Method Validation. U.S. Department of Health and Human Services Food and Drug Administration (2001)
21) Lown J. W., *Pharmacol. Ther.*, **60**, 185—214 (1993).
22) van Asperen J., van Tellingen O., Tijssen F., Schinkel A. H., Beijnen J. H., *Br. J. Cancer*, **79**, 108—113 (1999).

International Journal of Pharmaceutics 423 (2012) 401–409

Contents lists available at SciVerse ScienceDirect

International Journal of Pharmaceutics

journal homepage: www.elsevier.com/locate/ijpharm

Pharmaceutical nanotechnology

Evaluation of intracellular trafficking and clearance from HeLa cells of doxorubicin-bound block copolymers

Kumiko Sakai-Kato[a,*], Keiko Ishikura[a], Yuki Oshima[a], Minoru Tada[b], Takuo Suzuki[b], Akiko Ishii-Watabe[b], Teruhide Yamaguchi[c], Nobuhiro Nishiyama[d], Kazunori Kataoka[d,e], Toru Kawanishi[c], Haruhiro Okuda[a]

[a] Division of Drugs, National Institute of Health Sciences, 1-18-1 Kamiyoga, Setagaya-ku, Tokyo 158-8501, Japan
[b] Division of Biological Chemistry and Biologicals, National Institute of Health Sciences, 1-18-1 Kamiyoga, Setagaya-ku, Tokyo 158-8501, Japan
[c] National Institute of Health Sciences, 1-18-1 Kamiyoga, Setagaya-ku, Tokyo 158-8501, Japan
[d] Center for Disease Biology and Integrative Medicine, Graduate School of Medicine, The University of Tokyo, 7-3-1 Hongo, Bunkyo-ku, Tokyo 113-0033, Japan
[e] Department of Materials Engineering, Graduate School of Engineering, The University of Tokyo, 7-3-1 Hongo, Bunkyo-ku, Tokyo 113-8656, Japan

ARTICLE INFO

Article history:
Received 1 July 2011
Received in revised form
16 November 2011
Accepted 15 December 2011
Available online 23 December 2011

Keywords:
Doxorubicin-bound block copolymers
Intracellular trafficking
Confocal microscopy
Transporter
Endocytosis

ABSTRACT

New technologies are needed to deliver medicines safely and effectively. Polymeric nanoparticulate carriers are one such technology under investigation. We examined the intracellular trafficking of doxorubicin-bound block copolymers quantitatively and by imaging doxorubicin-derived fluorescence using confocal microscopy. The polymers were internalized by endocytosis and distributed in endosomal/lysosomal compartments and the endoplasmic reticulum; unlike free doxorubicin, the polymers were not found in the nucleus. Moreover, the ATP-binding cassette protein B1 (ABCB1) transporter may be involved in the efflux of the polymer from cells. This drug delivery system is attractive because the endogenous transport system is used for the uptake and delivery of the artificial drug carrier to the target as well as for its efflux from cells to medium. Our results show that a drug delivery system strategy targeting this endogenous transport pathway may be useful for affecting specific molecular targets.

1. Introduction

Recently, genomic drug discovery techniques, organic synthesis, and screening technologies have been used to develop molecularly targeted medicines, some of which are already being used clinically (Hopkins and Groom, 2002; Hughes, 2009). However, these new technologies do not necessarily lead to the introduction of new treatments because even when promising compounds are discovered by genomic drug discovery techniques, they often have harmful properties or are difficult to deliver to the target because they are relatively insoluble (Hopkins and Groom, 2002; Lipinski et al., 2001). New formulation technologies are being developed to enhance the effectiveness and safety of pharmaceutical products by focusing on improving the release, targeting, and stability of drugs within the body, so that the location and timing of their action in the living body can be controlled.

Nanotechnological advances have contributed to the development of new drug delivery system (DDS) products such as polymeric micelles and liposomes that range in size from several tens of nanometers to 100 nm (Ferrari, 2005). Some of these DDS products are already being marketed as innovative medical treatments (O'Brien et al., 2004), and the number being used in clinical trials has risen impressively in recent years (Hamaguchi et al., 2007; Kuroda et al., 2009; Matsumura et al., 2004). These nanoparticulates possess several unique advantages for drug delivery, including high drug-loading capacity, controlled drug release, and small size, which allows the drug to accumulate in pathological tissues such as tumors, which have increased vascular permeability (Nishiyama and Kataoka, 2006).

Polymeric micelles have received considerable attention recently as promising macromolecular carrier systems (Allen et al., 1999; Kataoka et al., 1993, 2001; Lavasanifar et al., 2002; Torchilin, 2002; Torchilin et al., 2003). Polymeric micelles are amphipathic systems in which a hydrophobic core is covered with an outer

Abbreviations: DDS, drug delivery system; PEG, polyethyleneglycol; RES, reticuloenodothelial system; EPR, enhanced permeability and retention; Dox, doxorubicin; DMEM, Dulbecco's modified Eagle's medium; FBS, fetal bovine serum; DLS, dynamic light scattering; AFM, atomic force microscopy; HBSS, Hank's balanced salt solution; ER, endoplasmic reticulum; ECFP, enhanced cyan fluorescent protein; Alexa-transferrin, Alexa Fluor 488 conjugate of transferrin; MTOC, microtubule-organizing center; ABCB1, ATP-binding cassette protein B1; MDR1, multidrug resistance 1; (PBS), phosphate-buffered saline; EDTA, ethylenediamine tetraacetic acid; SDS, sodium dodecyl sulfate; PVDF, polyvinylidene fluoride.

* Corresponding author. Tel.: +81 3 3700 9662; fax: +81 3 3700 9662.
E-mail address: kumikato@nihs.go.jp (K. Sakai-Kato).

0378-5173/$ – see front matter © 2011 Elsevier B.V. All rights reserved.
doi:10.1016/j.ijpharm.2011.12.022

shell consisting of hydrophilic macromolecules such as polyethylene glycol (PEG) chains. Polymeric micelles can both encapsulate medicine of high density and evade the foreign body recognition mechanism within the reticuloendothelial system (RES), and they show excellent retention in the blood (Illum et al., 1987). In addition, accurate size control of the nanoparticulates enables them to accumulate in cancerous tissue, owing to the increased permeability of tumor vessels due to the enhanced permeability and retention (EPR) effect (Matsumura and Maeda, 1986).

To maximize the efficacy and safety of DDS products, it is important to deliver these products to specific target cells and subcellular compartments. In the experiments reported here, we used confocal microscopy to study the intracellular trafficking of polymeric nanoparticulate carriers. The use of covalently bound fluorescent reagents as probes is gradually clarifying the internalization pathways and intracellular localizations of polymeric nanoparticulate carriers (Lee and Kim, 2005; Manunta et al., 2007; Murakami et al., 2011; Rejman et al., 2005; Richardson et al., 2008; Sahay et al., 2008; Savić et al., 2003). However, the excretion of the polymers from target cells after they have released the incorporated drugs has not yet been clarified in detail, although information about the clearance of carriers from cells is important from the perspective of safety. In this study, we examined the trafficking of a polymeric nanoparticulate carrier in detail, including the efflux of the polymers from cells to medium, by direct measurement of doxorubicin (Dox) covalently bound to the block copolymer. This technique avoids the necessity of considering the effects of exogenously tagged fluorescent probes on the intracellular trafficking.

Dox is one of the most effective available anticancer drugs in spite of its severe toxic effects, especially cardiotoxicity (Olson et al., 1988). As the carrier we used a PEG-poly(aspartic acid) block copolymer with covalently bound Dox (Fig. 1) (Yokoyama et al., 1999), because Dox has relevant hydrophobicity to form globular micelles by means of the hydrophobic interactions, and inherent fluorescence to investigate the intracellular trafficking of the carrier itself. Dox is partially covalently bound to the side chain of the aspartic acid (about 45% of aspartic acids), so that prepared Dox-conjugated block copolymers show good Dox entrapment efficiency possibly due to the π–π interaction between conjugated and incorporated Dox molecules (Bae and Kataoka, 2009; Nakanishi et al., 2001). Therefore, in this carrier system, there are two kinds of Dox; one is Dox covalently bound to block copolymers, and the other is free Dox which is incorporated in the inner core and has a pharmacological activity by its release from the inner core. The inner core of the micelles is greatly hydrophobic owing to the conjugated Dox, while the PEG of the outer layer prevents uptake by the RES. The resulting micelle effectively accumulates in tumor tissue by the EPR effect and shows much stronger activity than free Dox (Nakanishi et al., 2001). Because the block copolymer can form globular micelles by means of hydrophobic interactions with the conjugated Dox, as shown in Section 3.1, we used a carrier without incorporated free Dox to investigate the intracellular trafficking of the carrier itself. Furthermore, by quantifying directly the amount of Dox covalently bound to the polymers, we could measure the intracellular amount of the polymers.

2. Materials and methods

2.1. Cells and micelles

HeLa cells (Health Science Research Resources Bank, Osaka, Japan) were kept in Dulbecco's modified Eagle's medium (DMEM; Invitrogen Corp., Carlsbad, CA, USA) supplemented with 10% fetal bovine serum (FBS; Nichirei Biosciences Inc., Tokyo, Japan) and 100 U/mL penicillin/streptomycin (Invitrogen). Cells were grown in a humidified incubator at 37 °C under 5% CO_2. Dox-bound polymeric micelles and fluorescent dye (DBD)-labeled PEG-polyaspartate block copolymers partially modified with 4-phenyl-1-butanol were synthesized by Nippon Kayaku Co. Ltd. (Tokyo, Japan) (Nakanishi et al., 2001).

2.2. Physicochemical data of Dox-bound micelles

The diameters and distribution of micelles were determined by using dynamic light scattering (DLS; Zetasizer Nano ZS, Malvern, UK) at 25 °C. The micelles were dissolved in water and filtered through a 0.2-μm filter before measurement. Atomic force microscopy (AFM) measurements were conducted with a NanoWizard II (JPK Instruments, Berlin, Germany) at room temperature. Images were obtained in tapping mode using a commercial microcantilever with a spring constant of 150 N/m (Olympus Corporation, Tokyo, Japan). AFM images were processed with SPM image processing v. 3 software from JPK Instruments.

2.3. Quantitation of Dox-bound polymers in HeLa cells

The amounts of Dox-bound polymers in HeLa cells were determined by measuring the amount of doxorubicinone, which is released by acid hydrolysis of Dox-bound polymers (Fig. 1b). HeLa cells (1.5×10^5) were plated in 35-mm glass-bottom dishes coated with poly-L-lysine (Matsunami, Osaka, Japan) in DMEM containing 10% FBS and 100 U/mL penicillin/streptomycin. After incubation for two days (37 °C, 5% CO_2), the cells were exposed to 50 μg/mL Dox-bound polymers in culture medium. After the indicated durations, the cells were washed and kept in phosphate-buffered saline (PBS) or Hank's balanced salt solution (HBSS; Invitrogen). The cells were trypsinized with 0.25% trypsin-ethylenediamine tetraacetic acid (EDTA) (Invitrogen) and collected. Cells were then washed with PBS three times, and a small part of the cell suspension was used for cell counting. After centrifugation at 1000 rpm for 5 min, cell pellets were resuspended in 100 μL PBS, and the suspension was divided into two parts (50 μL was used with acid hydrolysis and 50 μL without) and stored at −80 °C until analysis. After thawing, the cell suspensions were disrupted by ultrasonic liquid processor (ASTRASON 3000, Misonix, NY, USA) for 1 min. Then, 50 μL of suspension was hydrolyzed by 0.5 N HCl at 50 °C for 15 h. After hydrolysis, samples were deproteinized with methanol, followed by centrifugation at 15,000 × *g* for 5 min at 4 °C. The supernatant was then neutralized with ammonium buffer, and evaporated to dryness under reduced pressure (Savant SpeedVac concentrator, Thermo Fisher Scientific, MA, USA). The residues were resuspended in 60% methanol, and the doxorubicinone released from the polymers by acid hydrolysis was quantified by ultra-high-performance liquid chromatography by using our previously reported method (Sakai-Kato et al., 2010) to determine the amount of intracellular Dox-bound polymers (Fig. 1b). The other 50 μL of cell suspension was treated in the same way but without the hydrolysis step to evaluate the amount of free doxorubicinone, that is, doxorubicinone not derived from Dox-bound polymers. The results of three independent experiments were averaged and analyzed statistically by *t*-test.

2.4. In vitro cytotoxicity

HeLa cell lines were evaluated in the present study. The HeLa cells were maintained in monolayer cultures in DMEM containing 10% FBS and 100 U/mL penicillin/streptomycin. WST-8 Cell Counting kit-8 (Dojindo, Kumamoto, Japan) was used for cell proliferation assay. 3000 cells of HeLa cell line in 100 μL of culture medium were plated in 96 well plates and were then incubated for 24 h at 37 °C. Serial dilutions of Dox-bound polymers, micelles incorporating free Dox or just free Dox were added, and the cells were incubated for 24

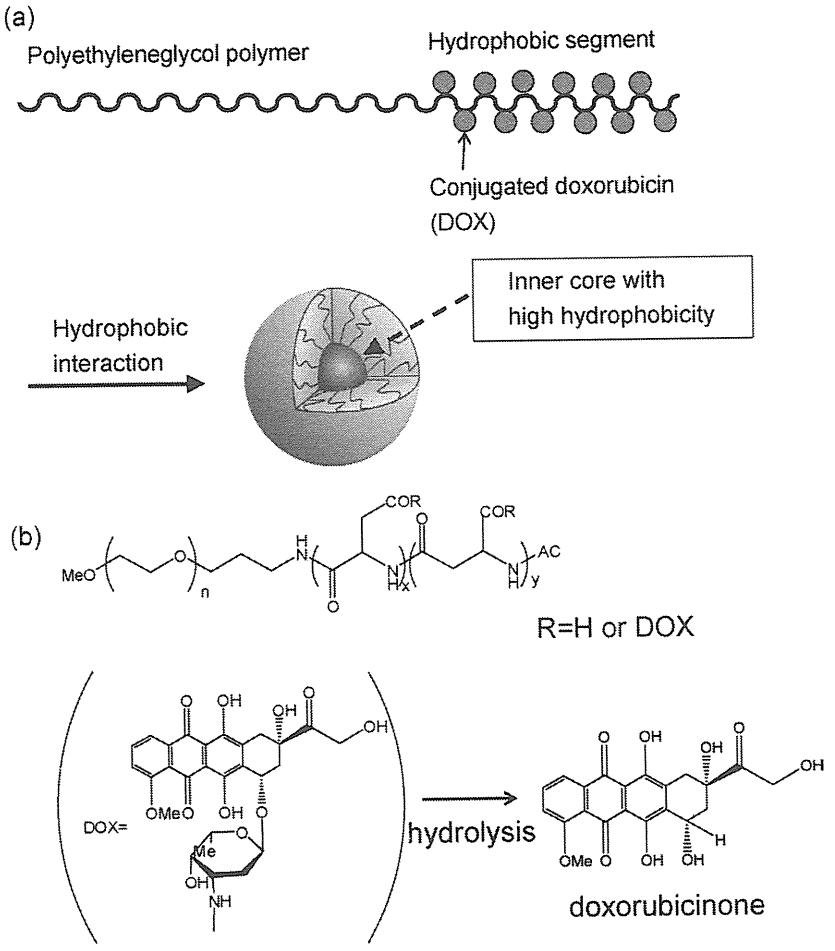

Fig. 1. Schematic of the structure of a Dox-bound polymeric micelle (a) and the chemical structure of the block copolymer (b). Polymer-bound Dox can be released as doxorubicinone by acid hydrolysis. The quantity of released doxorubicinone was used as a measure of the amount of intracellular polymers.

or 48 h. All data were expressed as mean ± SD of triplicate data. The data were then plotted as a percentage of the data from the control cultures, which were treated identically to the experimental cultures, except that no drug was added.

2.5. Confocal analysis of live cells

The intracellular trafficking of the Dox-bound micelles in live cells was examined by confocal microscopy (Carl Zeiss LSM 510, Oberkochen, Germany, or Nikon A1, Tokyo, Japan). Data were collected using dedicated software supplied by the manufacturers and exported as tagged image files (TIFs). HeLa cells (1.5×10^5) were plated in 35-mm glass-bottom dishes coated with poly-L-lysine (Matsunami) in DMEM containing 10% FBS and 100 U/mL penicillin/streptomycin. After incubation for two days (37 °C, 5% CO_2), the cells were exposed to 50 μg/mL Dox-bound polymers in culture medium. After the indicated durations, the cells were washed and kept in PBS or HBSS (Invitrogen) for imaging with the confocal microscope.

2.6. Labeling specific organelles in live cells

After incubation with Dox-bound polymers for 24 h, HeLa cells were washed with HBSS and labeled with organelle-specific fluorescent probes in accordance with the manufacturer's instructions. LysoTracker probe (Invitrogen) was used for labeling lysosomes, and ER-Tracker (Invitrogen) was used for labeling the endoplasmic reticulum (ER). A fluorescent Alexa Fluor 488 conjugate of transferrin (Alexa-transferrin; Invitrogen) was used as an exogenously added endocytic marker to delineate the endocytic recycling pathway for live cell imaging.

We also used an expression construct containing enhanced cyan fluorescent protein (ECFP) fused to an Golgi-targeting sequence derived from human β-1,4-galactosyltransferase as an Golgi localization marker (ECFP-Golgi). The construct was purchased from Clontech (Takara Bio Inc., Shiga, Japan). Cells were grown in 35-mm glass-bottom dishes coated with poly-L-lysine and transfected with Lipofectamine 2000 (Invitrogen). After overnight incubation, the cells were exposed to and allowed to internalize Dox-bound micelles for 24 h and then examined with confocal microscopy.

2.7. Efflux study of DOX-bound polymers or DBD-labeled polymers using the ABCB1 inhibitor verapamil

HeLa cells (1.5×10^5) were plated in 35-mm glass-bottom dishes coated with poly-L-lysine in DMEM containing 10% FBS and 100 U/mL penicillin/streptomycin. After incubation for two days (37 °C, 5% CO_2), the cells were exposed to 50 μg/mL Dox-bound polymers in culture medium for 3 h. Cells were washed with 50 μg/mL verapamil (Wako Pure Chemical Industries, Ltd., Osaka, Japan) (Davis et al., 2004; Kolwankar et al., 2005) or 0.1% dimethyl sulfoxide as a control. After washes, the cells were incubated for another 2 h in HBSS containing the same concentration of reagent. The cells were collected and processed for measurement of intracellular concentrations of Dox-bound polymers as described in Section 2.3. The efflux of DBD-labeled polymers was evaluated by

measurement of the fluorescent intensity inside cells using confocal microscopy. The intensity of the intracellular fluorescence was evaluated by image processing software (MetaMorph, Molecular Devices, CA, USA). The intensity of a single cell was mathematically determined by dividing the total intensity by the number of cells. Three independent experiments were averaged and analyzed statistically with the *t*-test.

2.8. Knockdown of ABCB1 by siRNA

Stealth RNAi oligonucleotides (Invitrogen) were used for siRNA experiments. Human ABCB1-siRNA sense, 5′-UCCCGUAGAAACCUUACAUUUAUGG-3′, and antisense, 5′-CCAUAAAUGUAAGGUUUCUACGGGA-3′, sequences were used. For a negative control, the Stealth RNAi Low GC Negative Control Duplex (Invitrogen) was used. The Stealth RNAi oligonucleotides were transfected into HeLa cells by using Lipofectamine RNAi MAX according to the manufacturer's protocols. After two days, the cells were exposed to 50 μg/mL Dox-bound polymers in culture medium for 3 h. After incubation, cells were washed with HBSS, and then incubated for another 2 h in HBSS without polymers. Cells were collected, and the intracellular polymers were quantified as described in Section 2.3.

2.9. Western blotting

Cells were washed with PBS and lysed in lysis buffer (20 mM Tris-HCl, pH 7.5; 1 mM EDTA; 10% glycerol; and 1% Triton X-100) containing protease inhibitors, namely, 2 mM phenylmethylsulfonyl fluoride and protease inhibitor cocktail (Sigma-Aldrich, St. Louis, MO, USA). Samples were electrophoresed on a sodium dodecyl sulfate (SDS)-polyacrylamide gel (5–20%) and transferred to a Polyvinylidene fluoride (PVDF) membrane. The blots were probed with anti-MDR (G-1) antibody (Santa Cruz Biotechnology, Inc., Santa Cruz, CA, USA) and developed with anti-mouse IgG peroxidase-linked species-specific whole antibody (from sheep) (GE Healthcare UK Limited, Little Chalfont, UK) by chemiluminescence.

3. Results and discussion

3.1. Physicochemical properties of Dox-bound micelles

The micelle carrier (Fig. 1) consisted of a block copolymer of PEG (molecular weight about 5000) and poly(aspartic acid) (polymerization degree, 30). To increase the hydrophobicity of the inner core, Dox was partially conjugated (about 45%) to the side chain of the aspartic acid. Because particle size affects the intracellular uptake of nanoparticulate formulations, we first examined the particle size of the micelles without free Dox. The Dox-bound micelles had a hydrodynamic diameter of about 42 nm at the dosed concentration of 50 μg/mL (Fig. 2a). AFM measurement of the micelles also confirmed that they were spherical with a particle size of around 40 nm (Fig. 2b). This size of micelle without free Dox is very similar to that of the micelles containing free Dox in the inner core that interacts with the conjugated Dox (Nakanishi et al., 2001), indicating that the presence of incorporated free Dox does not change the average diameter much.

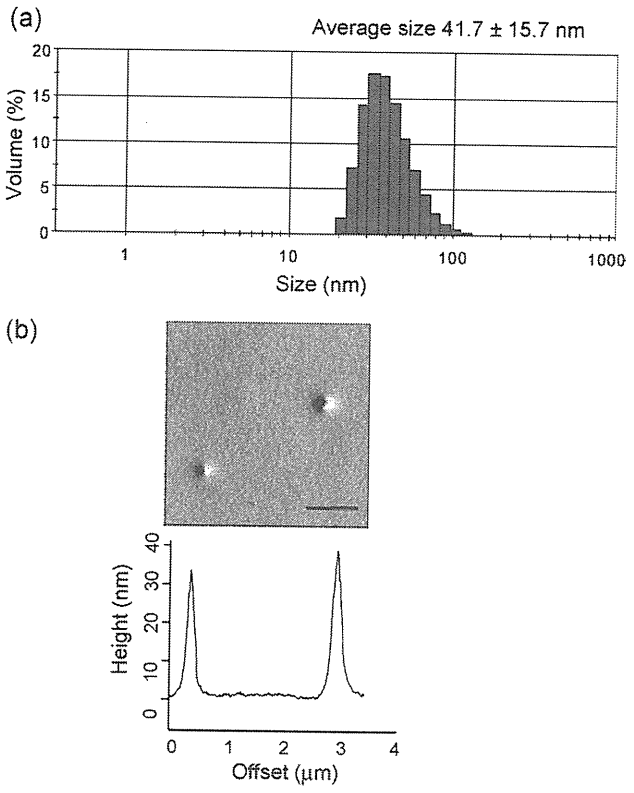

Fig. 2. Physicochemical properties of Dox-bound polymeric micelles. (a) Average size distribution of Dox-bound polymeric micelles by DLS. (b) The upper image shows an AFM image of Dox-bound polymeric micelles (bar: 1 μm) and the lower shows the cross-sectional topological profile of the image drawn in the upper panel.

3.2. In vitro cytotoxicity

We examined the *in vitro* cytotoxicity of the Dox-bound copolymers and the micelles incorporating free doxorubicin. As shown in Table 1, the cytotoxicity of doxorubicin-bound copolymers was negligible. This fact has been also reported in the previously published paper (Nakanishi et al., 2001). On the other hand, micelles incorporating free doxorubicin showed equivalent *in vitro* cytotoxic activity to free doxorubicin which is not incorporated into micelle. Therefore, in this system, the doxorubicin was conjugated to the block copolymer to increase the hydrophobicity of the inner core of the micelle so that efficient amount of free doxorubicin can be incorporated into the inner core of the micelles, and its cytotoxicity was negligible.

3.3. Intracellular uptake of Dox-bound polymers

To evaluate the intracellular uptake of Dox-bound polymers, we measured their intracellular amount by quantitating the doxorubicinone released from the intracellular polymers by acid hydrolysis treatment (Fig. 1b). Although the Dox-bound polymers contained 0.02% (w/w) free doxorubicinone as an impurity, no inherent free doxorubicinone was detected in the cells in any of the experiments in which we measured the intracellular concentration of doxorubicinone without acid hydrolysis. This result also indicates that

Table 1
IC50 values (μg/mL).

24 h			48 h		
Dox-bound polymer	Micelle incorporating free Dox	Free Dox	Dox-bound polymer	Micelle incorporating free Dox	Free Dox
>10	0.37	0.27	>10	0.045	0.024

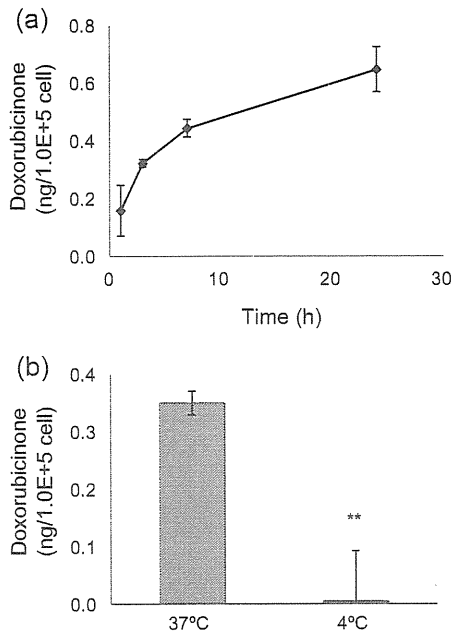

Fig. 3. Internalization of Dox-bound polymers. (a) Change in the internalized amount of Dox-bound polymers in cells as indicated by released doxorubicinone over time. HeLa cells were incubated in medium containing Dox-bound polymers for the indicated durations, followed by washes with PBS. The doxorubicinone released by acid hydrolysis was quantitated as a measure of the amount of intracellular polymers, as described in Section 2. (b) Effect of temperature on the internalization of Dox-bound polymers. HeLa cells were incubated in medium containing Dox-bound polymers at 37 °C or 4 °C for 3 h, followed by washes with PBS. The amount of intracellular polymers was quantitated by measuring the doxorubicinone released by acid hydrolysis, as described in Section 2. $^{**}P < 0.01$.

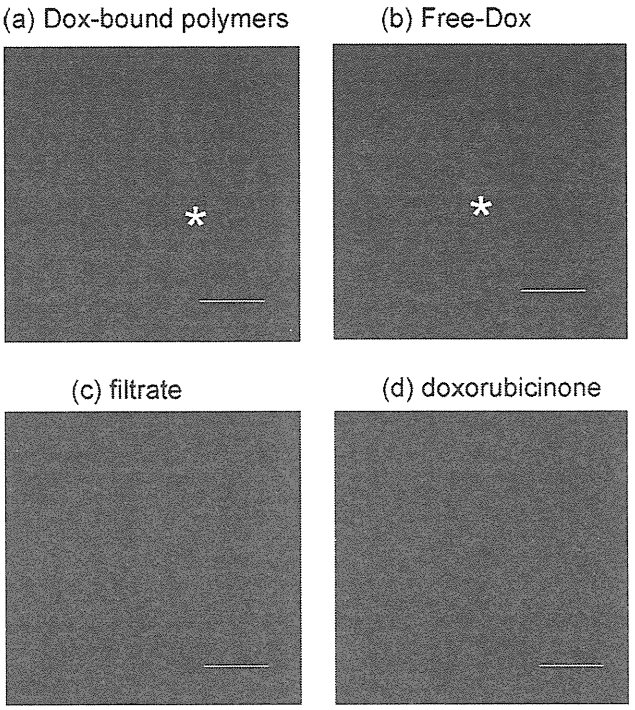

Fig. 4. Intracellular distribution of (a) DOX-bound polymers in HeLa cells exposed to 50 μg/mL Dox-bound polymers and (b) free DOX in cells exposed to 5 μg/mL free Dox for 1 h. Intracellular distribution of DOX-bound polymers in HeLa cells (c) cultured for 24 h in medium containing the filtrate of medium that was preincubated with Dox-bound polymers, and (d) cultured with 20 ng/mL free doxorubicinone for 24 h. Bars: 10 μm. Asterisk indicates the nucleus.

degradation of Dox-bound polymers that releases doxorubicinone during the experiments was negligible.

We then incubated HeLa cells in medium containing Dox-bound polymers for 1–24 h. After the incubation, the cells were washed. By determining the amounts of doxorubicinone released from Dox-bound polymers by acid hydrolysis of the cells, we were able to observe a time-dependent increase in the intracellular amount of Dox-bound polymers (Fig. 3a). Moreover, the amount of polymers in cells was significantly lower in cells incubated with the polymers at 4 °C than at 37 °C (Fig. 3b), indicating that the cells took up the polymers by endocytosis.

3.4. Intracellular distribution of Dox-bound polymers

The intracellular distribution of Dox-bound polymers was studied by confocal microscopy using the inherent fluorescence of the Dox covalently bound to the block copolymers. The Dox-bound polymers were localized in the perinuclear regions but not in the nucleus (Fig. 4a). This was different from the localization of free Dox which was distributed in the nucleus after 1 h (Fig. 4b), as reported previously (Beyer et al., 2001). This distribution will explain the fact that *in vitro* cytotoxicity of Dox-bound polymers was negligible (Table 1). To confirm that the Dox was not released from block copolymers as doxorubicinone (Fig. 1b) during the incubation time of the experiment, Dox-bound polymers were incubated in cell culture medium for 1 h at 37 °C, and then removed by centrifugal filtration using a Microcon YM-3 tube (Millipore, MA, USA). The resultant filtrate was added to the cell culture medium. Confocal microscopy showed no fluorescence within the cells (Fig. 4c). Furthermore, when HeLa cells were cultured in cell culture medium containing 20 ng/mL free doxorubicinone, which corresponds to 0.02% (w/w) of Dox-bound polymers, for 24 h, fluorescence was negligible within the cells (Fig. 4d). These results show that the fluorescence seen within the cells after Dox-bound polymer incubation is caused by the uptake of polymers and not by free doxorubicinone or Dox.

We next examined the intracellular localization of Dox-bound polymers by colocalization studies using fluorescent organelle markers. The fluorescence derived from Dox-bound polymers coincided well with the specific staining of the ER by ER-Tracker in double-labeling experiments (Fig. 5a). High-resolution images showed that both staining procedures clearly stained membranal structures (Fig. 5b).

Because the Golgi apparatus is also located in the perinuclear area and is involved in the intracellular transport of various molecules, we investigated the localization of the polymers by transfecting cells with an expression construct containing ECFP fused to a Golgi-specific protein. As shown in Fig. 5c, the distribution of polymers in the Golgi was negligible. We also confirmed that treatment of cells with Lipofectamine treatment did not affect the distribution of polymers (data not shown).

To what, then, can this particularly strong staining of the perinuclear areas be attributed? The perinuclear area is known to be the microtubule-organizing center (MTOC), an area in eukaryotic cells from which microtubules emerge and where endosomes and other endocytotic vesicles cluster (Matteoni and Kreis, 1987). In fact, a fluorescent staining image showed that the vesicles containing Dox-bound polymers in the perinuclear area (Fig. 6a, yellow arrows) coincided with the MTOC, as marked by Alexa-transferrin, an endocytic marker (Fig. 6a, white arrows). Some of the vesicles containing polymers were also stained by LysoTracker, a dye that specifically stains lysosomes (Fig. 6b). These results show that the polymers are internalized by endocytosis and transported to endosomal/lysosomal compartments. Duncan and colleagues, examined the localization of polymers by using Oregon Green as a fluorescent tag and found that three water-soluble polymeric carriers, *N*-(2-hydroxypropyl)methacrylamide, Dextran, and PEG, localized to late

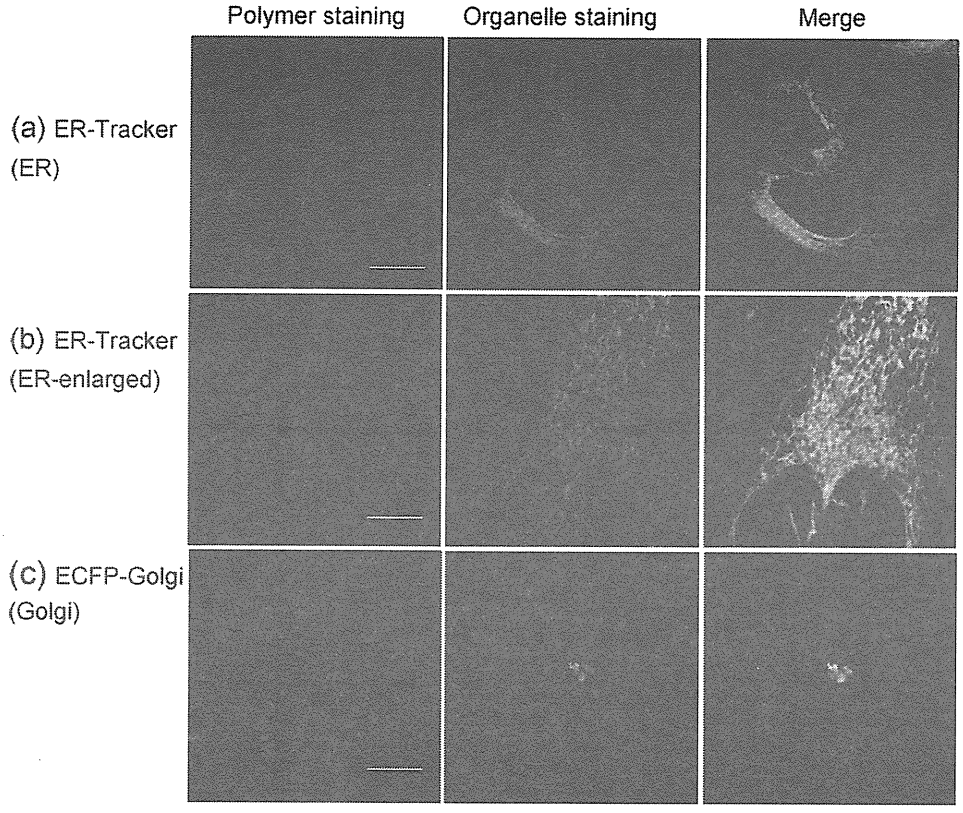

Fig. 5. Localization of Dox-bound polymers in cells co-stained with organelle-specific markers. Left, images of stained Dox-bound polymers; middle, organelle-specific fluorescent staining images; right, merged images of the left and middle images. Localization experiments using. (a and b) ER-Tracker for ER, (c) ECFP-Golgi for Golgi. Bars: 10 μm for (a) and (c). Bars: 5 μm for (b).

endosomal compartments (including lysosomes) (Richardson et al., 2008), findings consistent with our results. The perinuclear localization of the polymers is a great advantage of this system with regard to the incorporation of a nuclear-targeted drug or gene.

Most nanomaterials have been shown to exploit more than one pathway to gain cellular entry, and the pathway exploited can determine the intracellular fate (Sahay et al., 2010a). After internalization into HeLa cells, the Dox-bound polymers might be delivered to the ER directly from endosomes; in the case of cholesterol, there is some evidence for a direct pathway from endosomes to the ER (Ioannou, 2001; Mineo and Anderson, 2001). Or the polymers might be delivered to the ER directly, bypassing the endosomes/lysosomes, as do unimers of the amphiphilic triblock copolymer of poly(ethylene oxide), poly(propylene oxide), and Pluronic P85 (Sahay et al., 2010b). Simian virus 40 is known to enter the cytosol *via* the ER, suggesting that polymers distributed

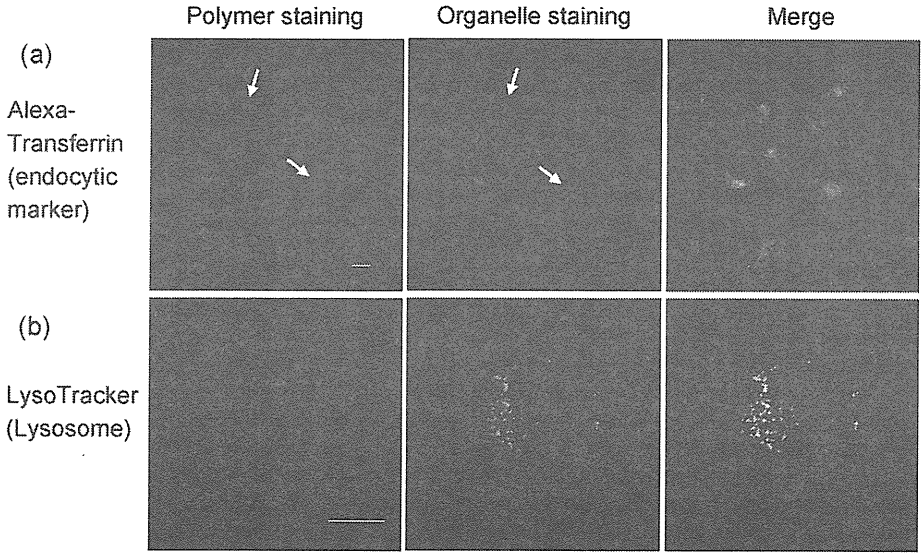

Fig. 6. Fluorescent staining images of Dox-bound polymers in cells co-stained with organelle-specific markers. Left, images of stained Dox-bound polymers; middle, organelle-specific fluorescent staining images; right, merged images of the left and middle images. Localization experiments using. (a) Alexa-transferrin, an endocytic compartment marker, and (b) LysoTracker, which is specific for lysosomes. Bars: 10 μm. Yellow and white arrows in (a) indicate the MTOC area.

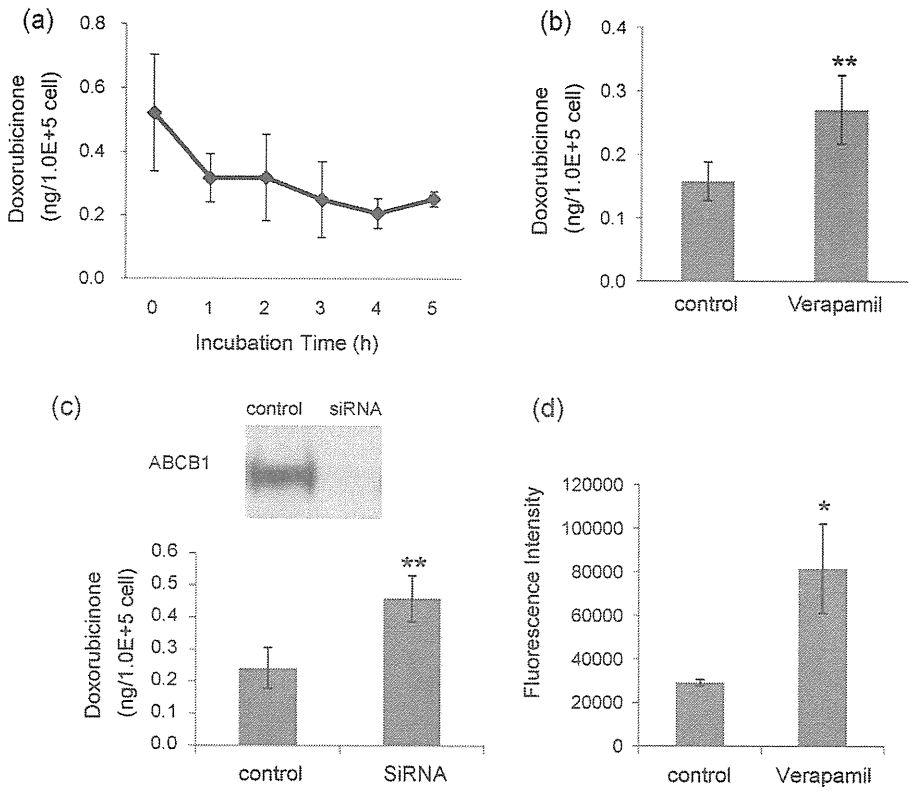

Fig. 7. Efflux of Dox-bound polymers. (a) Time-dependent change in intracellular Dox-bound polymers as indicated by released doxorubicinone. After incubation in medium with Dox-bound polymers, HeLa cells were washed and incubated with HBSS at 37 °C for the indicated durations. The doxorubicinone released by acid hydrolysis was quantitated as the amount of intracellular polymers as described in Section 2. (b) Effect of ABCB1 transporter on the efflux of Dox-bound polymers. HeLa cells were exposed to 50 μg/mL Dox-bound polymers in culture medium for 3 h. Cells were washed with 50 μg/mL verapamil or 0.1% dimethyl sulfoxide as a control. Then, the cells were incubated for another 2 h in HBSS containing the same concentration of each reagent. The amount of intracellular polymers was quantitated as the amount of doxorubicinone released by acid hydrolysis, as described in Section 2. $^{**}P < 0.01$. (c) Effect of the knockdown of ABCB1 transporter expression by siRNA on the efflux of Dox-bound polymers. Expression of ABCB1 in cell extracts was analyzed by immunoblot analysis (top). After 2 days of siRNA transfection, the cells were exposed to 50 μg/mL of Dox-bound polymers in culture medium for 3 h. After incubation, the cells were washed with HBSS and then incubated for another 2 h in HBSS without polymer. The amount of intracellular polymers was quantitated as the amount of doxorubicinone released by acid hydrolysis, as described in Section 2 (bottom). $^{**}P < 0.01$. Effect of ABCB1 transporter on the efflux of DBD-labeled polymers. HeLa cells were exposed to 50 μg/mL DBD-labeled polymers in culture medium for 24 h. Cells were washed with 50 μg/mL verapamil or 0.1% dimethyl sulfoxide as a control. Then, the cells were incubated for another 2 h in HBSS containing the same concentration of each reagent. The fluorescence intensity in a single cell was calculated as described in Section 2. $^{*}P < 0.05$.

in the ER might similarly gain access to the cytosol (Damm et al., 2005). The characteristic distribution pattern of the polymers did not change much with increasing incubation times from 0.5 to 24 h (data not shown). Although it is not clear whether the polymers maintain their structure as globular micelles or exist as unimers after internalization into a cell, increasing the dosed polymer concentration to 1 mg/mL did not change the staining pattern (data not shown). Recently, we showed PEG and poly(glutamic acid) block copolymer micelles incorporating dichloro(1,2-diaminocyclohexane)platinum(II) selectively dissociate within late endosomes (Murakami et al., 2011), suggesting that the Dox-bound polymers might also dissociate.

3.5. *Efflux of Dox-bound polymers from HeLa cells to medium*

As described in Section 3.2, the amount of intracellular Dox-bound polymers increased with time when cells were continuously exposed to Dox-bound polymers (Fig. 3a). In contrast, the amount of Dox-bound polymers gradually decreased after the Dox-bound polymers were removed from the medium (Fig. 7a). Interestingly, this decrease in the intracellular amount of Dox-bound polymers was abolished in the presence of verapamil, an inhibitor of ABCB1 (ATP-binding cassette protein B1) transporter (Fig. 7b). The ABCB1 transporter, which is also known as multidrug resistance 1 (MDR-1) or P-glycoprotein, is a member of the ABC-type transporter family and an efflux pump for various drugs. To further investigate the role of this transporter in the efflux of Dox-bound polymers from cells to medium, small interference RNAs (siRNAs) were used to target ABCB1 RNA in HeLa cells. Two days after transfection of synthetic siRNA, Western blot analysis showed that levels of ABCB1 protein expression in siRNA-transfected HeLa cells were drastically decreased (Fig. 7c), and the efflux of Dox-bound polymers from these cells was also significantly inhibited (Fig. 7c). The efflux of DBD-labeled polymers was also inhibited by ABCB1 transporter inhibitor, when intracellular fluorescent intensity of DBD-labeled polymers was measured (Fig. 7d). These results suggest that ABCB1 transporter is a key regulator of the clearance of Dox-bound polymers from HeLa cells.

It is reported that drug-binding site of ABCB1 transporter is located at a drug binding pocket that is formed by transmembrane segments and allow access of molecules directly from the membranes (Aller et al., 2009; Loo et al., 2003a,b). Furthermore, it is also known that subdomains of the ER form close contact with plasma membrane and some proteins may regulate the formation of direct membrane contacts that facilitate sterol exchange between the ER and plasma membrane (Ikonen, 2008).

Therefore, it is probable that a part of Dox-bound polymers localized in ER are transported to plasma membrane and then recognized at the drug binding site in the transmembrane segments of ABCB1 transporter.

In general, the ABCB1 transporter has very broad substrate specificity: recent studies have shown that it mediates the efflux

of a relatively large peptide, amyloid β peptide (molecular weight, 4.5 kDa), across the blood–brain barrier into the bloodstream (Cirrito et al., 2005; Kuhnke et al., 2007; Lam et al., 2001). To the best of our knowledge, the ABCB1 transporter has not been reported before to be involved in the clearance of block copolymers from cells. Because ABCB1 transporter is expressed primarily in certain normal cell types in the liver, kidney, and jejunum (Thiebaut et al., 1987), the role of ABCB1 transporter as excretion pump of Dox-bound polymer and the effect of ABCB1 transporter on the polymer blood level are probably significant from a safety perspective.

Taken together, the findings presented here suggest that Dox-bound polymers are incorporated by endocytosis. Some of the incorporated polymers are transferred to the endosome/lysosome system, and the rest may bypass the endosomal system. Then, the polymers are likely delivered to other compartments, including ER and the plasma membrane. The excretion of excess polymers from the cells is mediated by the ABCB1 transporter. Although in this system, the conjugated Dox was not designed to be released from the polymers, our results concerning intracellular trafficking and clearance of polymers would be very useful to design the carrier system where bound drugs are released from the carrier for pharmacological activity.

4. Conclusion

We investigated the intracellular trafficking of Dox-bound polymers. The polymers are internalized into cells by endocytosis, then transported to endosomal/lysosomal compartments, followed by partial distribution to the ER, or transported directly to the ER. The active excretion of the polymers from the cells may be mediated by the ABCB1 transporter. It is surprising that cells utilize their endogenous transport system for intracellular trafficking of this artificial drug carrier. Our results potentially can contribute not only to the discussion of safety issues of polymeric therapeutics but also the development of a DDS strategy utilizing or targeting this endogenous pathway more effectively.

Acknowledgements

The authors are grateful for support from Research on Publicly Essential Drugs and Medical Devices (Japan Health Sciences Foundation), a Health Labor Sciences Research Grant, and the Global COE Program for the Center for Medical System Innovation, MEXT, KAKENHI (21790046), and Nippon Kayaku Co. Ltd. We thank Mr. R. Nakamura (Nikon Corp.) for technical assistance.

References

Allen, C., Maysinger, D., Eisenberg, A., 1999. Nano-engineering block copolymer aggregates for drug delivery. Colloids Surf. B: Biointerfaces 16, 3–27.

Aller, S.G., Yu, J., Ward, A., Weng, Y., Chittaboina, S., Zhuo, R., Harrell, P.M., Trinh, Y.T., Zhang, Q., Urbatsch, I.L., Chang, G., 2009. Structure of P-glycoprotein reveals a molecular basis for poly-specific drug binding. Science 323, 1718–1722.

Bae, Y., Kataoka, K., 2009. Intelligent polymeric micelles from functional poly (ethylene glycol)-poly (amino acid) block copolymers. Adv. Drug Deliv. Rev. 61, 768–784.

Beyer, U., Rothern-Rutishauser, B., Unger, C., Wunderli-Allenspach, H., Kratz, F., 2001. Differences in the intracellular distribution of acid-sensitive doxorubicin-protein conjugates in comparison to free and liposomal formulated doxorubicin as shown by confocal microscopy. Pharm. Res. 18, 29–38.

Cirrito, J.R., Deane, R., Fagan, A.M., Spinner, M.L., Parsadanian, M., Finn, M.B., Jiang, H., Prior, J.L., Sagare, A., Bales, K.R., Paul, S.M., Zlokovic, B.V., Piwnica-Worms, D., Holtzman, D.M., 2005. P-glycoprotein deficiency at the blood-brain barrier increases amyloid-beta deposition in an Alzheimer disease mouse model. J Clin. Invest. 115, 3285–3290.

Damm, E.M., Pelkmans, L., Kartenbeck, J., Mezzacasa, A., Kurzchalia, T., Helenius, A., 2005. Clathrin- and caveolin-1-independent endocytosis: entry of simian virus 40 into cells devoid of caveolae. J. Cell Biol. 168, 477–488.

Davis, B.M., Humeau, L., Slepushkin, V., Binder, G., Korshalla, L., Ni, Y., Ogunjimi, E.O., Chang, L.F., Lu, X., Dropulic, B., 2004. ABC transporter inhibitors that are substrates enhance lentiviral vector transduction into primitive hematopoietic progenitor cells. Blood 104, 364–373.

Ferrari, M., 2005. Cancer nanotechnology: opportunities and challenges. Nat. Rev. Cancer 5, 161–171.

Hamaguchi, T., Kato, K., Yasui, H., Morizane, C., Ikeda, M., Ueno, H., Muro, K., Yamada, Y., Okusaka, T., Shirao, K., Shimada, Y., Nakahama, H., Matsumura, Y., 2007. A phase I and pharmacokinetic study of NK105, a paclitaxel-incorporating micellar nanoparticle formulation. Br. J. Cancer 97, 170–176.

Hopkins, A.L., Groom, C.R., 2002. The druggable genome. Nat. Rev. Drug Discov. 1, 727–730.

Hughes, B., 2009. Gearing up for follow-on biologics. Nat. Rev. Drug Discov. 8, 181.

Ikonen, E., 2008. Cellular cholesterol trafficking and compartmentalization. Nat. Rev. Mol. Cell Biol. 9, 125–138.

Illum, L., Davis, S.S., Müller, R.H., Mak, E., West, P., 1987. The organ distribution and circulation time of intravenously injected colloidal carriers sterically stabilized with a blockcopolymer-poloxamine 908. Life Sci. 40, 367–374.

Ioannou, Y.A., 2001. Multidrug permeases and subcellular cholesterol transport. Nat. Rev. Mol. Cell Biol. 2, 657–668.

Kataoka, K., Kwon, G.S., Yokoyama, M., Okano, T., Sakurai, Y., 1993. Block copolymer micelles as vehicles for drug delivery. J. Control. Rel. 24, 119–132.

Kataoka, K., Harada, A., Nagasaki, Y., 2001. Block copolymer micelles for drug delivery: design, characterization and biological significance. Adv. Drug Deliv. Rev. 47, 113–131.

Kolwankar, D., Glover, D.D., Ware, J.A., Tracy, T.S., 2005. Expression and function of ABCB1 and ABCG2 in human placental tissue. Drug Metab. Dispos. 33, 524–529.

Kuhnke, D., Jedlitschky, G., Grube, M., Krohn, M., Jucker, M., Mosyagin, I., Cascorbi, I., Walker, L.C., Kroemer, H.K., Warzok, R.W., Vogelgesang, S., 2007. MDR1-P-glycoprotein (ABCB1) mediates transport of Alzheimer's amyloid-β peptides – implications for the mechanisms of Aβ clearance at the blood–brain barrier. Brain Pathol. 17, 347–353.

Kuroda, J., Kuratsu, J., Yasunaga, M., Koga, Y., Saito, Y., Matsumura, Y., 2009. Potent antitumor effect of SN-38-incorporating polymeric micelle, NK012, against malignant glioma. Int. J. Cancer 124, 2505–2511.

Lam, F.C., Liu, R., Lu, P., Shapiro, A.B., Renoir, J.-M., Sharom, F.J., Reiner, P.B., 2001. β-Amyloid efflux mediated by p-glycoprotein. J. Neurochem. 76, 1121–1128.

Lavasanifar, A., Samuel, J., Kwon, G.S., 2002. Poly(ethylene oxide)-block-poly (L-amino acid) micelles for drug delivery. Adv. Drug Deliv. Rev. 54, 169–190.

Lee, S.M., Kim, J.S., 2005. Intracellular trafficking of transferrin-conjugated liposome/DNA complexes by confocal microscopy. Arch. Pharm. Res. 28, 93–99.

Lipinski, C.A., Lombardo, F., Dominy, B.W., Feeney, P.J., 2001. Experimental and computational approaches to estimate solubility and permeability in drug discovery and development settings. Adv. Drug Deliv. Rev. 46, 3–26.

Loo, T.W., Bartlett, M.C., Clarke, D.M., 2003a. Substrate-induced conformational changes in the transmembrane segments of human P-glycoprotein. J. Biol. Chem. 278, 13603–13606.

Loo, T.W., Bartlett, M.C., Clarke, D.M., 2003b. Methanethiosulfonate derivatives of rhodamine and verapamil activate human P-glycoprotein at different sites. J. Biol. Chem. 278, 50136–50141.

Manunta, M., Izzo, L., Duncan, R., Jones, A.T., 2007. Establishment of subcellular fractionation techniques to monitor the intracellular fate of polymer therapeutics. II. Identification of endosomal and lysosomal compartments in HepG2 cells combining single-step subcellular fractionation with fluorescent imaging. J. Drug Target. 15, 37–50.

Matsumura, Y., Maeda, H., 1986. A new concept for macromolecular therapeutics in cancer chemotherapy: mechanism of tumoritropic accumulation of proteins and the antitumor agent smancs. Cancer Res. 46, 6387–6392.

Matsumura, Y., Hamaguchi, T., Ura, T., Muro, K., Yamada, Y., Shimada, Y., Shirao, K., Okusaka, T., Ueno, H., Ikeda, M., Watanabe, N., 2004. Phase I clinical trial and pharmacokinetic evaluation of NK911, a micelle-encapsulated doxorubicin. Br. J. Cancer 91, 1775–1781.

Matteoni, R., Kreis, T.E., 1987. Translocation and clustering of endosomes and lysosomes depends on microtubules. J. Cell Biol. 105, 1253–1265.

Mineo, C., Anderson, R.G., 2001. Potocytosis. Robert Feulgen lecture. Histochem. Cell Biol. 116, 109–118.

Murakami, M., Cabral, H., Matsumoto, Y., Wu, S., Kano, M.R., Yamori, T., Nishiyama, N., Kataoka, K., 2011. Improving drug potency and efficacy by nanocarrier-mediated subcellular targeting. Sci. Transl. Med. 3, 64ra2.

Nakanishi, T., Fukushima, S., Okamoto, K., Suzuki, M., Matsumura, Y., Yokoyama, M., Okano, T., Sakurai, Y., Kataoka, K., 2001. Development of the polymer micelle carrier system for doxorubicin. J. Control. Rel. 74, 295–302.

Nishiyama, N., Kataoka, K., 2006. Current state, achievements, and future prospects of polymeric micelles as nanocarriers for drug and gene delivery. Pharmacol. Ther. 112, 630–648.

O'Brien, M.E.R., Wigler, N., Inbar, M., Rosso, R., Grischke, E., Santoro, A., Catane, R., Kieback, D.G., Tomczak, P., Ackland, S.P., Orlandi, F., Mellars, L., Alland, L., Tendler, C., 2004. Reduced cardiotoxicity and comparable efficacy in a phase III trial of pegylated liposomal doxorubicin HCl (CAELYX™/Doxil®) versus conventional doxorubicin for first-line treatment of metastatic breast cancer. Ann. Oncol. 15, 440–449.

Olson, R.D., Mushlin, P.S., Brenner, D.E., Fleischer, S., Cusack, B.J., Chang, B.K., Boucek Jr., R.J., 1988. Doxorubicin cardiotoxicity may be caused by its metabolite, doxorubicinol. Proc. Natl. Acad. Sci. U.S.A. 85, 3585–3589.